JACS
JOURNAL OF THE AMERICAN CHEMICAL SOCIETY
Article
pubs.acs.org/JACS

Using Reduced Catalysts for Oxidation Reactions: Mechanistic Studies of the "Periana-Catalytica" System for CH_4 Oxidation

Oleg A. Mironov,[†] Steven M. Bischof,[‡] Michael M. Konnick,[‡] Brian G. Hashiguchi,[‡] Vadim R. Ziatdinov,[†] William A. Goddard, III,[§] Mårten Ahlquist,[§] and Roy A. Periana*[,‡]

[†]Loker Hydrocarbon Research Institute, University of Southern California, University Park, Los Angeles, California 90089, United States

[‡]The Scripps Energy & Materials Center, The Scripps Research Institute, 130 Scripps Way #3A1, Jupiter, Florida 33458, United States

[§]Materials and Process Simulation Center, California Institute of Technology, Pasadena, California 91125, United States

Supporting Information

ABSTRACT: Designing oxidation catalysts based on CH activation with reduced, low oxidation state species is a seeming dilemma given the proclivity for catalyst deactivation by overoxidation. This dilemma has been recognized in the Shilov system where reduced Pt^{II} is used to catalyze methane functionalization. Thus, it is generally accepted that key to replacing Pt^{IV} in that system with more practical oxidants is ensuring that the oxidant does not over-oxidize the reduced Pt^{II} species. The "Periana-Catalytica" system, which utilizes (bpym)-$Pt^{II}Cl_2$ in concentrated sulfuric acid solvent at 200 °C, is a highly stable catalyst for the selective, high yield oxy-functionalization of methane. In lieu of the over-oxidation dilemma, the high stability and observed rapid oxidation of (bpym)$Pt^{II}Cl_2$ to Pt^{IV} in the absence of methane would seem to contradict the originally proposed mechanism involving CH activation by a reduced Pt^{II} species. Mechanistic studies show that the originally proposed mechanism is incomplete and that while CH activation does proceed with Pt^{II} there is a solution to the over-oxidation dilemma. Importantly, contrary to the accepted view to minimize Pt^{II} overoxidation, these studies also show that increasing that rate could increase the rate of catalysis and catalyst stability. The mechanistic basis for this counterintuitive prediction could help to guide the design of new catalysts for alkane oxidation that operate by CH activation.

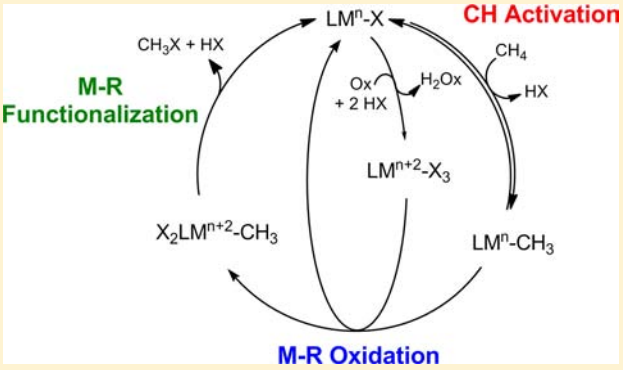

INTRODUCTION

The direct conversion of primary feedstocks, such as alkanes, to fuels and chemicals at lower temperatures with high selectivity is an important on going challenge in catalysis.[1] Homogeneous catalysts based on the CH activation reaction are among the most effective for this transformation. The seminal homogeneous system developed by Shilov (eq 1) has shown this as a possible reality for the selective functionalization of CH_4 to CH_3OH and CH_3Cl.[2] The Shilov system operated in aqueous HCl at <100 °C with low CH_4 conversions using $[Pt^{IV}Cl_6]^{2-}$ as the overall oxidant. Extensive studies by Shilov,[3] Bercaw,[4] and others[5] have provided strong support for a reduced, homogeneous Pt^{II} species that reacts with CH_4 via the CH activation reaction to generate $Pt^{II}-CH_3$ intermediates.

$$CH_4 + [Pt^{IV}Cl_6]^{2-} \xrightarrow{[Pt^{II}Cl_4]^{2-}} CH_3X + [Pt^{II}Cl_4]^{2-} + HX \quad (1)$$

It is notable that the more labile, reduced Pt^{II}, and not oxidized Pt^{IV} species is proposed to be active for CH activation of CH_4. Generally, coordination of the CH bond of an alkane is a key prerequisite to generate the M−C bond via subsequent CH cleavage. Consequently, as alkanes are extremely poor ligands, the reduced complex, LM^n, can be much more effective at CH activation than the more oxidized states, $LM^{>n}$. Indeed, most of the well-established CH activation systems are with lower oxidation state metal complexes.[1]

However, it would seem paradoxical to design catalysts for hydrocarbon oxidation reactions that are based on CH activation with reduced oxidation states, LM^nX, of the catalyst. Thus, as shown in Scheme 1, if the higher oxidation-state species, $LM^{>n}$-X, is both more stable and inactive for the CH activation, the irreversible oxidation of the reduced species, LM^n-X, should lead to deactivation when the catalyst pools as the higher oxidized species, $LM^{>n}$-X. This issue did not exist in the Shilov system as the overall Pt^{IV} oxidant could not consume $[Pt^{II}]$, as this oxidant itself becomes Pt^{II} upon oxidation. However, in practical systems, the stoichiometric oxidant

Received: May 22, 2013
Published: August 8, 2013

   dx.doi.org/10.1021/ja404895z | J. Am. Chem. Soc. 2013, 135, 14644−14658

Scheme 1. General Catalytic Cycle for RH Oxidation Where Only the Reduced Form of the Catalyst Is Active for CH Activation

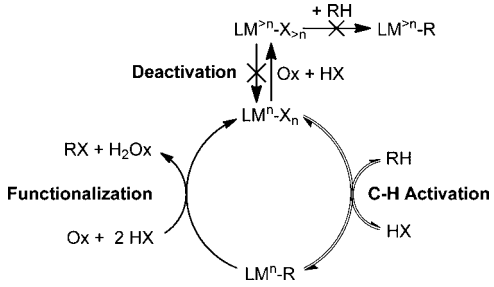

cannot be the higher oxidation state of the catalyst as these are typically expensive metals.[6] Furthermore, carrying out the oxidation of CH_4 to CH_3OH ($E^o \sim -0.6$ V, eq 2),[7] requires that the overall oxidant in Scheme 1, Ox, must be both relatively strong ($E^o > 0.6$ V) and present in large excess relative to the catalyst (for turnover number (TON) to be >1). Under these conditions, it would seem unlikely to prevent deactivation from oxidation of the reduced state of the catalyst that is. This potential issue has been recognized by several researchers. In particular, Bercaw, noted that replacement of Pt^{IV} in the Shilov system with more practical overall oxidants require, "strict constraints on suitable alternative oxidants; although they must be fast enough to oxidize [Pt^{II}-R] competitively with protonolysis, they must **not**[8] rapidly oxidize inorganic Pt^{II}, i.e., $[Pt^{II}Cl_n(H_2O)_{4-n}]_{2-n}$, since that would deplete the [reduced oxidation state][9] species responsible for alkane activation."[10] Indeed, the identification of catalysts and practical oxidants that meet this requirement for slow oxidation of the reduced catalytic species that is active for CH activation is an important consideration of ongoing research.[11]

$$CH_4 + H_2O \rightarrow CH_3OH + 2H^+ + 2e^- \quad (E^0 < \sim 0.6V) \tag{2}$$

Herein, we report on studies of the highly efficient Periana-Catalytica catalyst system that oxidizes CH_4 to CH_3OH in high yield (eq 3). This system is well suited for study as CH activation of methane is proposed with a reduced Pt^{II} species despite the high stability of the system (TONs of 500 were

Scheme 2. Plausible Pathways For the Periana-Catalytica System That May Account for the High Stability

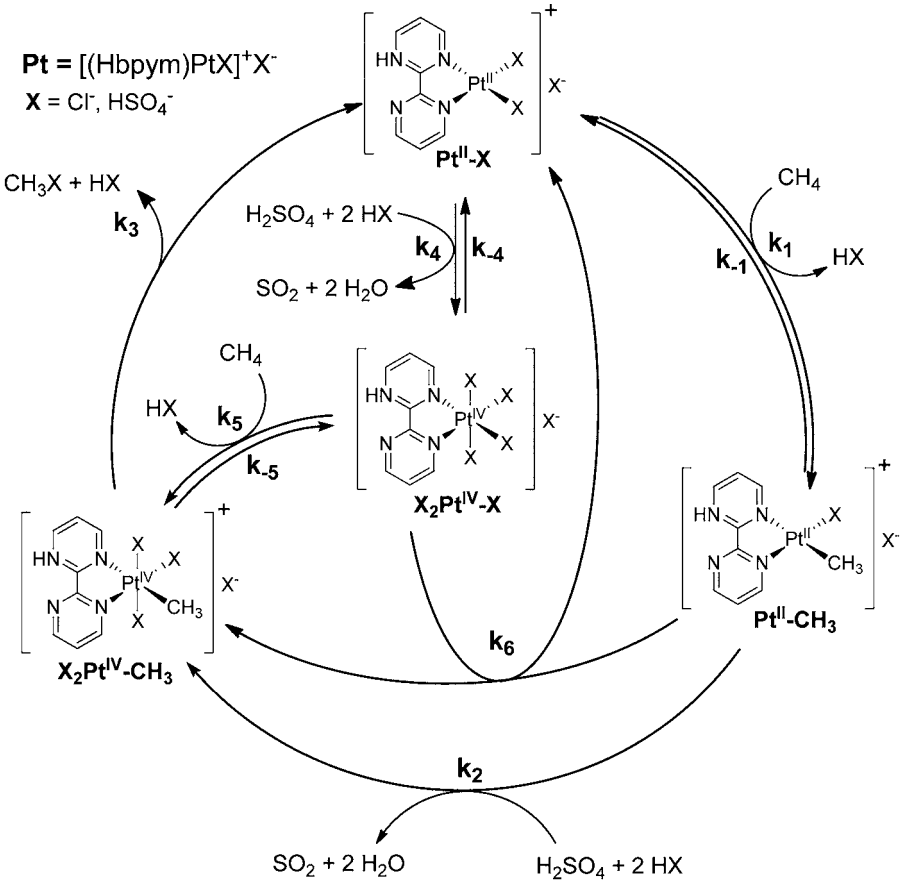

Catalytic Pathways Studied

A: k_1, k_2, k_3, k_4 *(CH Activation by* ***Pt^{II}-X****, k_1; Irreversible generation of* ***X$_2$Pt^{IV}-X****, k_4)*
B: k_4, k_5, k_3 *(CH Activation by* ***X$_2$Pt^{IV}-X****, k_5)*
C: k_4, k_{-4}, k_1, k_2, k_3 *(CH Activation by* ***Pt^{II}-X****, k_1; Reversible generation of* ***X$_2$Pt^{IV}-X****, k_4)*
D: k_1, k_4, k_6, k_3 *(CH Activation by* ***Pt^{II}-X****, k_1; Rapid Oxidation of* ***Pt^{II}-Me*** *by* ***X$_2$Pt^{IV}-X****, k_6)*

dx.doi.org/10.1021/ja404895z | J. Am. Chem. Soc. 2013, 135, 14644−14658

reported without deactivation)[12]) and reaction conditions of 220 °C in strongly oxidizing 101% H_2SO_4 (eq 4) as the solvent. It has been generally considered that the stability of the system resulted from meeting the accepted requirement of oxidizing the Pt^{II}–CH_3 intermediate faster than the non-methylated, reduced, Pt^{II} catalyst. Significantly, our studies now show that this is not the basis for the high stability and that catalysis proceeds by a more complex mechanism. We believe that these new findings could provide important guidance in the design of new catalysts for direct, selective alkane oxidation. It should be noted that the mechanism for catalyst stability could be different from that for product formation and that both operate at steady state. It is also possible that a single pathway is responsible for both catalyst stability and product formation. These possibilities are examined and discussed herein.

$$CH_4 + H_2SO_4 \xrightarrow[H_2SO_4,220°C]{(bpym)PtCl_2} CH_3OH + SO_2 + H_2O \quad (3)$$

$$2SO_3(g) + 2H^+ + 2e^- \rightarrow SO_2 + H_2SO_4(l) \quad (E \sim 1V) \quad (4)$$

RESULTS AND DISCUSSION

The Periana-Catalytica system utilizes a Pt^{II} complex, (bpym)-$Pt^{II}Cl_2$ (bpym = 2,2′-bipyrimidinyl) as the catalyst for the selective oxidation of CH_4 in H_2SO_4 to generate a mixture of CH_3OH, $CH_3OH_2^+$, and CH_3OSO_3H (this mixture will be referred to herein as CH_3X) and SO_2. In addition to the high stability, the system is highly efficient for carrying out the oxidation reaction. After 3 h, at 220 °C, with 500 psig of CH_4, in concentrated H_2SO_4 (101%, ~19 M), a TOF of $\sim 10^{-3}$ s^{-1} with ~70% yield of CH_3X based on added CH_4 at >90% selectivity and a volumetric productivity of $\sim 10^{-7}$ mol cc^{-1} s^{-1} was observed.[13] A basis for reaction by CH activation was the observation that catalysis in D_2SO_4 led to H/D exchange with methane. This observation combined with reported studies of the Shilov system[6] provided the basis for the proposed mechanism based on CH activation with a Pt^{II} rather than Pt^{IV} species. While several theoretical studies of this system have been performed, no detailed experimental studies of the reaction mechanism have been reported to date. Consistent with the original reports, we found that the system is very efficient and remained homogeneous with no observable Pt black or insoluble species after reaction. The thermodynamic values of a $\Delta H^{\ddagger}$ of 34 ± 2 kcal/mol and a $\Delta S^{\ddagger}$ of −3.8 ± 0.8 eu ($\Delta G^{\ddagger}$ 36 ± 2.5 kcal/mol at 220 °C) were experimentally obtained for the overall reaction in eq 3.

To more fully understand the basis for the high stability of the system, we examined the original as well as several other plausible, independent mechanisms. These mechanisms are shown in Scheme 2, as Pathways A, (the original pathway), B, C, and D involving only the reaction steps shown in the inset for each pathway. Each pathway is intended to be considered as a separate mechanism that is independent of the others. This composite diagram of the various steps is used to emphasize the common and variable steps between the four pathways. As can be seen, on the basis of reported theoretical studies, the (bpym)$PtCl_2$ in liquid H_2SO_4 is proposed to generate various protonated forms, where Pt is used to designate the (Hbpym)PtX motif.[14]

Pathway A. Pathway A is the mechanism proposed by the original investigators involving steps k_1, k_2, and k_3 with the added consideration of the irreversible oxidation of **Pt^{II}-X** to **X_2Pt^{IV}-X**, step k_4. Key characteristics of this pathway are that CH activation of CH_4 involves reaction with **Pt^{II}-X** to generate **Pt^{II}-CH_3** in step k_1, oxidation of **Pt^{II}-CH_3** to **X_2Pt^{IV}-CH_3** by concentrated H_2SO_4 solvent in step k_2 followed by reductive functionalization of **X_2Pt^{IV}-CH_3** to CH_3X and **Pt^{II}-X**, step k_3. Consideration of step k_4 in Pathway A is the fundamental basis for this study.

Our studies show that the reaction is first order in methane and catalyst (Figures 1 and 2). The reactions with methane

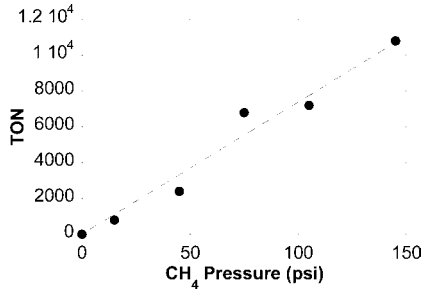

Figure 1. TON versus CH_4 pressure. Conditions: 5 mM Pt(bpym)Cl_2, 10–145 psi CH_4, 10 mL 98% D_2SO_4, 40 min, 165 °C.

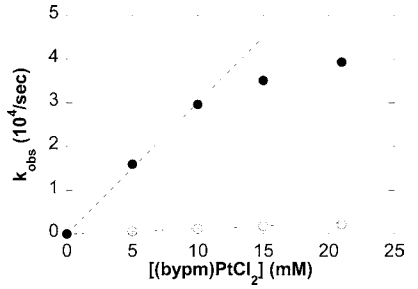

Figure 2. k_{obs} of H/D exchange (●) and MeOH production (○) versus [Pt(bpym)Cl_2]. Conditions: [Pt(bpym)Cl_2] = 5–21 mM, 500 psi CH_4, 10 mL 98% D_2SO_4, 60 min, 165 °C.

were carried out with 5 mM **Pt^{II}** in order to operate outside of the mass transfer limited regime. With the reactor system utilized in these studies, control studies show that the reaction becomes mass transfer limited above ~10 mM **Pt^{II}-X**, and we believe that this the basis for the deviation from linearity from the reaction rate versus [**Pt^{II}**] (Figure 2). The rate of H/D exchange between D_2SO_4 solvent and CH_4 was also shown to be highly dependent on the proton activity of the H_2SO_4 solvent ($-H_0$) (Figure 3). The reaction can be followed above $-H_0$ of ~8 (85% H_2SO_4), however, due to inaccuracies in the detection limits of our analytical methods we could not follow

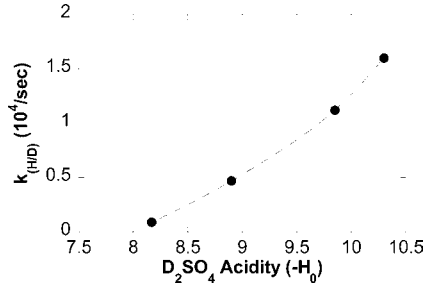

Figure 3. k_{obs} H/D exchange vs $-H_0$. Conditions: 5 mM Pt(bpym)Cl_2, 500 psi CH_4, 10 mL of 85–98% D_2SO_4, 60 min, 165 °C.

dx.doi.org/10.1021/ja404895z | J. Am. Chem. Soc. 2013, 135, 14644–14658

the reaction below this level of acidity. ^{1}H and ^{13}C NMR spectroscopic analysis of the crude liquid phase after catalysis with 100% labeled $^{13}CH_4$ in concentrated H_2SO_4 or D_2SO_4 showed no resonances that could be assigned to Pt-$^{13}CH_3$ species, and all the $^{13}CH_3$ resonances observed were from dissolved $^{13}CH_4$ and the various forms of $^{13}CH_3X$. The resonances in the region for the bpym ligand could not be analyzed due to the various multiprotonated species present in solution and proton exchange.

To examine whether the **Pt^{II}-X** species proposed for CH activation could be oxidized to **$X_2Pt^{IV}X$** by step k_4 in Scheme 2, a 10 mM solution of (bpym)$Pt^{II}Cl_2$ in 98% H_2SO_4 was heated to 200 °C under N_2 (in the absence of CH_4) for 1 h. The color of the reaction mixture changed from orange to yellow[15] (see SI for N_2 vs CH_4 pictures),[16] and ∼110% ± 20% of SO_2 (based on eq 5) was observed in the gas phase. The SO_2 was identified by gas chromatography and quantified by titrimetric methods based on SO_2 trapping in H_2O_2(aq) solution (to form H_2SO_4) and back-titrated with KOH(aq). Control experiments demonstrated that SO_2 is not generated without the Pt^{II}-complex or from the bypm ligand alone. Attempts at analysis by *in situ* ^{1}H and ^{13}C NMR studies were complicated by poorly resolved, overlapping resonances, *vide supra*. Similarly, after numerous attempts at examining **Pt^{II}-X** in H_2SO_4, no ^{195}Pt-NMR resonances could be clearly observed. This was not unexpected, as this system was designed to be highly labile and changing of "X" groups on Pt-centers drastically change the chemical shift (i.e., *cis*-$Pt(NH_3)_2Cl_2$: δ −2168 ppm vs *cis*-$Pt(NH_3)_2(OH)_2$: δ −1590 ppm),[17] exacerbating the broadening of signals. Attempts at characterizing the proposed (bpym)$PtCl_2(HSO_4)_2$ species by isolation or derivativization were unsuccessful due to the high solubility of the reaction product, the low volatility and reactive properties of concentrated sulfuric acid. Although there are other explanations for the stoichiometric formation of SO_2 from **Pt^{II}-X**, these results would suggest that the oxidation of Pt^{II} to Pt^{IV} is quantitative and effectively irreversible ($k_4 \gg k_{-4}$) in the absence of CH_4.

$$(\text{bypm})PtCl_2 + 3H_2SO_4 \rightarrow (\text{bpym})PtCl_2(HSO_4)_2 + SO_2 + 2H_2O \quad (5)$$

If one assumes that catalysis proceeds via Pathway A, the high observed stability of the system would require that the rate of irreversible oxidation of **Pt^{II}-X** required for CH activation to presumed inactive **X_2-Pt^{IV}-X**, (i.e., k_4) be substantially slower than the overall rate of catalysis for generation of CH_3X. In this case, the system could exhibit apparent high stability as any catalyst deactivation could be sufficiently slow and undetectable over the time required to observe the reported 500 TONs.[13] Assuming that **Pt^{II}-X** is the resting state, this would require that the activation barrier for the oxidation to **X_2-Pt^{IV}-X** be substantially higher than the ∼36 kcal/mol activation barrier for overall catalysis.

To obtain rate data on the oxidation of **Pt^{II}-X**, we attempted to follow the reaction by the rate of SO_2 formation; however, this was hampered by lack of reproducibility that resulted from the high solubility of SO_2 in H_2SO_4 coupled with technical challenges with mass transfer between the gas and liquid phases. The observation that SO_2 formation after 1 h is negligible at <150 °C but stoichiometric at 220 °C, *vide supra*, would suggest a barrier of >30 but <36 kcal/mol for the reaction. To obtain a better approximation of the activation barrier, we examined the reaction by DFT calculations. Ziegler[18] reported that the oxidation of **Pt^{II}-X** with SO_3 is endoergic by 8.3 kcal/mol with a barrier of 35.1 kcal/mol. Attesting to the difficulty in modeling reactions under the catalytic conditions, our calculations of the Ziegler mechanism showed an inaccessible barrier of 44 kcal/mol. However, consistent with the interpretation of the experimental data on the oxidation of **Pt^{II}-X**, we found an alternative pathway for the oxidation of **Pt^{II}-X** to **$X_2Pt^{IV}X$** with a barrier of ∼36 kcal/mol and a ΔG_{rxn} of −1 to −6 kcal/mol, depending on whether the oxidant was presumed to be H_2SO_4 or $H_2S_2O_7$, respectively (see SI).

The results show that the rate of oxidation of Pt^{II} to Pt^{IV} is comparable to that for overall catalysis. Under these circumstances, if the catalytic mechanism for product formation operated by Pathway A involving only steps k_1−k_3, deactivation by step k_4 should occur in minutes, as effectively all of the reduced, **Pt^{II}-X** catalytic species that are active for CH activation would pool as presumed inactive, more stable **X_2Pt^{IV}-X**. Given the high stability of the system, this would suggest that either Pathway A does not operate or is not a complete description of the system. It should be emphasized that these observations do not rule out the possibility that Pathway A is solely or partially the basis for product formation, while other reactions account for the high stability.

Pathway B. As seen in Scheme 2, Pathway B involves only steps k_4, k_5, and k_3. The key distinction from Pathways A, C, or D is that CH activation is with a Pt^{IV} species, **X_2Pt^{IV}-X**, (rather than **Pt^{II}-X**) to directly generate **X_2Pt^{IV}-CH_3**. This is followed by k_3 to generate **Pt^{II}-X** and the product CH_3X. Reoxidation of **Pt^{II}-X** by H_2SO_4, step k_4, regenerates the **X_2Pt^{IV}-X**. The key basis for considering this pathway is that deactivation of the catalytic system is less likely if CH activation was carried out by the more stable, high-oxidation-state species, **X_2Pt^{IV}-X**. We were particularly interested in this pathway as it seems the simplest basis for the high stability. Indeed, most efficient homogeneous catalyst systems identified to date for the efficient oxidation of CH_4 to CH_3OH operate by CH activation with high-oxidation states of the catalyst, e.g., Pd^{II},[19] $Au^{I/III}$,[20] Hg^{II},[21] etc. Additionally, it is known that Pt^{IV} species are competent for CH activation of aromatics in CF_3CO_2H.[22] While alkanes are more poorly coordinating than arenes, it is plausible that alkanes could coordinate with Pt^{IV} centers by a dissociative mechanism in poorly coordinating concentrated H_2SO_4 at 220 °C. Reported calculations showing that the barrier for CH activation with Pt^{IV} species is $\Delta G^{\ddagger}$ = 41 ± 2 kcal/mol[23] suggests that such a pathway is not viable.[24] However, discrepancies in reported calculations, *vide supra*, are likely a result of the highly polar, poorly coordinating, strongly oxidizing, and strongly hydrogen-bonding characteristics of concentrated H_2SO_4 at 220 °C. This increases the likelihood of highly charged species being involved and suggests that CH activation by Pt^{IV} should not be ruled out.

To examine the possibility of CH activation by the higher oxidations state species, **X_2-Pt^{IV}-X**, the catalytic reaction was carried starting with a Pt^{IV} model complex. The expectation was that if the original proposal, Pathway A, of CH activation by the lower oxidation state species, **Pt^{II}-X**, was correct, an induction period may be observed that would rule against Pathway B. However, the lack of an induction period could not be interpreted, as it is well-known that that Pt^{IV} can readily decomposes to or contaminated with Pt^{II}.[25] *In situ* synthesis of (bpym)$Pt^{IV}X_4$ (X = Cl or HSO_4) by mixing $Pt^{IV}(OH)_4(H_2O)_2$,

dx.doi.org/10.1021/ja404895z | J. Am. Chem. Soc. 2013, 135, 14644−14658

bpym, and HCl in a 1:1:2 molar ration was used as one model of $\mathbf{X_2Pt^{IV}}$-**X** (see SI for details). Interestingly, these reactions gave the same results as starting with the Pt^{II} catalyst, (bpym)$PtCl_2$. Moreover, no induction period was observed. As noted above, while this is consistent with Pt^{IV} as a catalyst, this result is inconclusive. Therefore additional evidence is required to provide stronger support for this pathway.

To more definitively investigate the possibility for CH activation by $\mathbf{X_2Pt^{IV}X}$, Pathway B, we examined the stoichiometric reaction of a model complex of the predicted intermediate, $\mathbf{X_2Pt^{IV}}$-$\mathbf{CH_3}$, with concentrated D_2SO_4 at 180 °C, Scheme 3. The model complex of $\mathbf{X_2Pt^{IV}}$-$\mathbf{CH_3}$ utilized in this

Scheme 3. Kinetic Analysis Assuming Pathway B

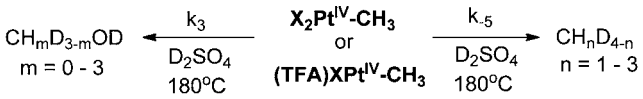

$$\left(\frac{\frac{d[CH_nD_{4-n}]}{dt}}{\frac{d[CH_mD_{3-m}X]}{dt}}\right)_{CAT} = \left[\frac{(\text{mol } CH_nD_{4-n})}{(\text{mol } CH_mD_{3-m}X)}\right]_{CAT} = \frac{k_{-5}[\mathbf{X_2Pt^{IV}}\text{-}\mathbf{CH_3}][D_2SO_4]}{k_3[\mathbf{X_2Pt^{IV}}\text{-}\mathbf{CH_3}][D_2SO_4]} = \frac{k_{-5}}{k_3}$$

$$\left(\frac{\frac{d[CH_nD_{4-n}]}{dt}}{\frac{d[CH_mD_{3-m}X]}{dt}}\right)_{(TFA)XPt^{IV}\text{-}CH_3} = \left[\frac{(\text{mol } CH_nD_{4-n})}{(\text{mol } CH_mD_{3-m}X)}\right]_{(TFA)XPt^{IV}\text{-}CH_3} = \frac{k_{-5}[(\mathbf{TFA})\mathbf{XPt^{IV}}\text{-}\mathbf{CH_3}][D_2SO_4]}{k_3[(\mathbf{TFA})\mathbf{XPt^{IV}}\text{-}\mathbf{CH_3}][D_2SO_4]} = \frac{k_{-5}}{k_3}$$

study was the fully characterized (bpym)$Pt^{IV}(CH_3)(TFA)Cl_2$, (**TFA**)(**X**)-$\mathbf{Pt^{IV}}$-$\mathbf{CH_3}$. This complex has the same bpym ligand as the actual catalyst, (bpym)$PtCl_2$, and differs from $\mathbf{X_2Pt^{IV}}$-$\mathbf{CH_3}$ only by the presence of a TFA anion. Given the expected rapid loss of TFA in hot H_2SO_4, it is reasonable that (**TFA**)(**X**)-$\mathbf{Pt^{IV}}$-$\mathbf{CH_3}$ is a good model of the proposed intermediate in Pathway B, $\mathbf{X_2Pt^{IV}}$-$\mathbf{CH_3}$. Consistent with $\mathbf{X_2Pt^{IV}}$-$\mathbf{CH_3}$ as an intermediate in catalysis, carrying out the catalysis starting with (**TFA**)(**X**)-$\mathbf{Pt^{IV}}$-$\mathbf{CH_3}$ showed identical results to starting with (bpym)$PtCl_2$.

As noted in the original work, carrying out the catalysis in D_2SO_4 led to significantly more D incorporation into methane than generation of methanol, eq 6. If the reaction proceeded by Pathway B, this would suggest that the CH activation is reversible, i.e., k_5 and k_{-5} is fast compared to the conversion of $\mathbf{X_2Pt^{IV}}$-$\mathbf{CH_3}$ to the functionalized product (k_3). As can be seen in Scheme 3, kinetic analysis of Pathway B would predict that the molar ratio of all the isotopologues of methane, to methanol, $[(\text{mol } CH_nD_{4-n}])/(\text{mol } CH_mD_{3-m}X)]_{CAT}$, generated from catalytic reaction of CH_4 in D_2SO_4 would give k_{-5}/k_3, where CAT is used to designate data obtained from the actual catalytic system. This analysis assumes that steps k_5 and k_3 are first order in $\mathbf{X_2Pt^{IV}}$-$\mathbf{CH_3}$[26] and (**TFA**)(**X**)-$\mathbf{Pt^{IV}}$-$\mathbf{CH_3}$ and carried out at low conversions of CH_4 and D_2SO_4 to ensure pseudofirst-order kinetics and irreversible formation of the reaction products. This analysis assumes first order dependence on D_2SO_4. However, this is not required for comparison of $[(\text{mol } CH_nD_{4-n}])/(\text{mol } CH_mD_{3-m}X)]$ obtained from the catalytic reaction and the reaction of the model complex (**TFA**)(**X**)-$\mathbf{Pt^{IV}}$-$\mathbf{CH_3}$ (*vide infra*), since the comparison is carried out under identical conditions.

$$CH_4 + D_2SO_4 \xrightarrow[D_2SO_4,180°C]{(bpym)PtCl_2} CH_nD_{4-n} + CH_mD_{3-m}OD + SO_2 + D_2O \quad (6)$$

The key hypothesis is that if Pathway B was the mechanism of catalysis, then the stoichiometric reaction of independently synthesized (**TFA**)(**X**)-$\mathbf{Pt^{IV}}$-$\mathbf{CH_3}$ under the same reaction conditions would give $[(\text{mol } CH_nD_{4-n}])/(\text{mol } CH_mD_{3-m}X)]_{Pt(IV)\text{-}CH_3}$ (where the Pt(IV)-CH_3 is used to designate the ratio of products obtained from the stoichiometric reaction of (**TFA**)(**X**)-$\mathbf{Pt^{IV}}$-$\mathbf{CH_3}$) that is the same or comparable to $[(\text{mol } CH_nD_{4-n}])/(\text{mol } CH_mD_{3-m}X)]_{CAT}$ from the catalytic reaction of CH_4 carried out in D_2SO_4. Conversely, any large mismatch between these ratios, while not definitive, would rule against Pathway B as the catalytic mechanism and the basis for the stability of the system. Significantly, the comparison shown in Scheme 3 is only possible, if the reactions are irreversible and the ratio of products is independent of the concentration of $\mathbf{X_2Pt^{IV}}$-$\mathbf{CH_3}$ and reaction time. This is essential since the concentration and reactions times with the model complex are almost certainly different for the presumed intermediate, $\mathbf{X_2Pt^{IV}}$-$\mathbf{CH_3}$, in the actual catalytic system. It should be noted that there are some differences between the catalytic and stoichiometric studies as SO_2 (albeit this was shown to have no effect on the catalytic reaction, *vide infra*), and other Pt-species could be present in the actual catalytic reaction.

To obtain $[(\text{mol } CH_nD_{4-n}])/(\text{mol } CH_mD_{3-m}X)]_{CAT}$, the catalytic system with CH_4 was examined as previously described, but using concentrated D_2SO_4, eq 6. The reactions were examined between 160 and 190 °C with 5 mM of (bpmy)$Pt^{II}Cl_2$ at <10% conversion of added CH_4 to ensure pseudofirst-order conditions with respect to both CH_4 and D_2SO_4. Consistent with the original work, analysis of the gas phase from the reaction in D_2SO_4 showed H/D exchange between D_2SO_4 and CH_4 to generate the various isotopologues of CH_nD_{4-n} ($n = 0 - 4$). Temperature-dependent studies show that $\Delta H^{\ddagger} = 28 \pm 2$ kcal/mol, $\Delta S^{\ddagger} = -11 \pm 3$ eu, and $\Delta G^{\ddagger} = 33 \pm 2$ kcal/mol at 180 °C were obtained for this H/D exchange reaction. The $CH_mD_{3-m}X$ ($m = 0$ and 3) was quantified by GC/MS analysis. As can be seen in Table 1, entry 1 the molar ratio, $(\text{mol } CH_nD_{4-n}])/(\text{mol } CH_mD_{3-m}X)]_{CAT}$, was ~20.

The stoichiometric reactions of the model complex were carried out by injecting 0.1 mL of a 1.04 M solution of (**TFA**)(**X**)-$\mathbf{Pt^{IV}}$-$\mathbf{CH_3}$, in DMSO all at once into a glass vial

Table 1. Ratio of Isotopologues of Methane and Methyl Bisulfate from Reactions in D_2SO_4[a]

entry	reactants	$(\text{mol } [CH_nD_{4-n}])/(\text{mol } [CH_mD_{3-m}X])$[b]
1	catalytic conditions (CH_4 + D_2SO_4 + (bpym)$Pt^{II}Cl_2$)	~20
2	**TFA-Pt^{IV}-CH$_3$**	<0.01
3	**TFA-Pt^{II}-CH$_3$**	~20
4[c]	**Pt^{IV}** + **TFA-Pt^{II}-CH$_3$**	<0.01
5[d]	**CH$_4$** + **D$_2$SO$_4$** + **Pt^{IV}** + (bpym)$Pt^{II}Cl_2$	~0.03

[a]All reactions were carried out at 180 °C in 19 M D_2SO_4. With each Pt complexes at 10 mM for all experiments, except entry 5. [b]Sum of all the isotopologues, $n = 1-3$ and $m = 0-3$. [c]1 equiv of Pt^{IV} relative to (bpym)$PtCl_2$ as a mixture of $Pt(H_2O)_2(OH)_4$, bpym, and $ClSO_3H$. [d]5 equiv of Pt^{IV}.

dx.doi.org/10.1021/ja404895z | J. Am. Chem. Soc. 2013, 135, 14644−14658

under argon containing 5 mL of a stirred solution of concentrated D_2SO_4 at 180 °C.[27] Immediately after injection, the vials were removed, cooled to RT, and the gaseous and liquid phases were analyzed by GC-MS and ^1H NMR. Remarkably, these studies showed that even in concentrated D_2SO_4 at 180 °C, no CH_nD_{4-n} was observed (by GS/MS) from the stoichiometric reaction of **(TFA)(X)-Pt^{IV}-CH$_3$** and the predominant product was $CH_mD_{3-m}X$ in essentially quantitative yield, $[(\text{mol } CH_nD_{4-n}])/([\text{mol } CH_mD_{3-m}X)]_{(TFA)Pt(IV)-CH_3} < 0.01$ (Table 1, entry 2). Significantly, this result is dramatically different from the molar ratio of products (~20) obtained from the catalytic reaction of CH_4 in D_2SO_4 with(bpym)$PtCl_2$ Table 1, entry 1. The poor correlation provides strong evidence that CH activation does not proceed via the Pt^{IV} complex (k_5) in Pathway B (Scheme 2). This is consistent with the difference between the ~31 kcal/mol barrier for H/D exchange from experiment and the ~41 kcal/mol barrier for CH activation by **X$_2$Pt^{IV}-X** obtained from DFT studies.[21] These results would suggest that it is unlikely that Pathway B involving CH activation by **X$_2$Pt^{IV}-X** accounts for the high stability of the system. Importantly, while these results rule against Pathway B, the facile, functionalization reaction of **TFA-Pt^{IV}-CH$_3$** to CH_3X provides strong support for the feasibility of the reductive functionalization step, k_3. Similar functionalization reactions were observed in model studies of the expected Pt^{IV}-CH_3 species in the Shilov system. The model complexes utilized in those studies contained ligands not present in this system and were carried out with different solvents and under much milder conditions.[6]

Pathway C. Pathway C involves only k_4, k_{-4}, k_1–k_3 in Scheme 2. Pathway C operates by CH activation with **Pt^{II}-X**. The key distinction is that, consistent with the experimental studies that shows complete oxidation of **Pt^{II}-X** upon treatment with hot D_2SO_4, **X$_2$Pt^{IV}-X** is an off-cycle species and assumed to be the resting state of the catalyst. Under reaction conditions, the resulting stability of the catalytic system could arise from equilibrium between **X$_2$Pt^{IV}-X** and a very low concentration of **Pt^{II}** (eq 7, $k_4/k_{-4} \gg 1$) that is an extremely active catalyst. This proposal could be consistent with our calculations that show this reaction is favorable but with a low ΔG_{rxn} from −1 to −6 kcal/mol, *vide supra*. As shown in Scheme 4, if the reaction proceeded by Pathway C involving only steps k_4, k_{-4}, k_1–k_3, it is logical that an increase in $[SO_2]$ would increase the equilibrium concentration of **Pt^{II}-X** and increase the rate of catalysis for formation of CH_nD_{4-n} or $CH_mD_{3-m}X$ (assuming that SO_2 has no impact on the other reaction steps in Pathway C).[28] To investigate this possibility, we examined the impact of added SO_2 on the catalytic rate. The reactions were carried out by comparing reactions as described in the original reports with the same $[D_2SO_4]$ (or H_2SO_4), [(bpym)-$PtCl_2$], temperature, and P_{CH_4} with and without 200 psig of SO_2 at the start of reaction. The results showed no difference in initial rates (<10% conversion) for formation of CH_nD_{4-n} or $CH_mD_{3-m}X$. These observations rule against Pathway C, Scheme 2, as the basis for the stability of the system. While there could be many explanations for the lack of change with increased $[SO_2]$, a plausible explanation is that **Pt^{II}-X**, rather than off-cycle **X$_2$Pt^{IV}-X**, is the resting state and active catalyst. In this case, changes in $[SO_2]$ would result in very small changes of [**Pt^{II}-X**] and increases in reaction rate that could not be observed.

Scheme 4. Kinetic Analysis of Pathway C Showing the Expected Dependence of Rate of Formation of Products (CH_nD_{4-n} or $CH_mD_{3-m}X$) on $[SO_2]$

$$\text{rate} \propto [\mathbf{Pt^{II}\text{-}X}][CH_4][H_2SO_4]$$

$$Pt^{II} = k_4/k_{-4}[(bpym)PtCl_2][SO_2][H_2O]^2[H_2SO_4]^{-3}$$

$$\text{rate} \propto k_4/k_{-4}\,[(bpym)PtCl_2][CH_4][SO_2][H_2O]^2[H_2SO_4]^{-2}$$

$$\mathbf{Pt^{II}\text{-}X} + 3H_2SO_4 \underset{k_{-4}}{\overset{k_4}{\rightleftharpoons}} \mathbf{X_2Pt^{IV}\text{-}X} + SO_2 + 2H_2O$$

$$X = HSO_4 \qquad (7)$$

Pathway D. Pathway D involves only steps, k_4, k_1, k_6, and k_3 in Scheme 2. In this mechanism, the CH activation step, k_1, involves reversible reaction of **Pt^{II}-X** with CH_4 to generate **Pt^{II}-CH$_3$**. **X$_2$Pt^{IV}-X** is assumed to be inactive for CH activation. A key aspect of Pathway D is that step k_6 provides a basis for the stability of the system. In this "self-repair" step, **X$_2$Pt^{IV}-X** is continuously generated from oxidation of **Pt^{II}-X** (eq 7) with concentrated H_2SO_4 and is brought back into the catalytic cycle by reaction with **Pt^{II}-CH$_3$** (eq 8). This reaction is similar to the Shilov system where at ~60 °C, Pt^{IV} is used as the stoichiometric oxidant that upon reduction generates the active Pt^{II} catalyst. The key difference is that the concentrated H_2SO_4 solvent (rather than **XPt^{IV}-X**) at 220 °C is the overall oxidant and that Pt^{IV} is continuously generated during catalysis. To be the basis for the stability of the system, it is critical that step k_6 operates at comparable or faster rates to step k_4. If the resting state of the catalyst is **Pt^{II}-X** and step k_6 is much slower than step k_4, all the catalyst would pool as **X$_2$Pt^{IV}-X** in minutes, and catalysis will effectively stop.

$$\mathbf{X_2Pt^{IV}\text{-}X} + \mathbf{Pt^{II}\text{-}CH_3} \xrightarrow[H_2SO_4]{} MeX + 2\mathbf{Pt^{II}\text{-}X} \qquad (8)$$

For step k_6 to be comparable to step k_4, it would require that k_6 be exceedingly large. Based on calculations that show the CH activation step, k_1, is endoergic with ΔG = ~16 kcal/mol, the concentration of the proposed **Pt^{II}-CH$_3$** intermediate from step k_1 should be vanishingly small. To be competitive with the oxidation of **Pt^{II}-X** (maximum concentration of 10 mM based on added (bpym)$PtCl_2$) by the H_2SO_4 solvent (k_4) and the protonolysis **Pt^{II}-CH$_3$**, (k_{-1}), the bimolecular reaction between **X$_2$Pt^{IV}-X** and **Pt^{II}-CH$_3$** in step k_6 would likely have to proceed with a barrier of <10 kcal/mol. Stoichiometric reactions between Pt^{IV} and Pt^{II}-CH_3 models of the Shilov system have been shown to rapidly generate CH_3X at rates that are competitive with protonolysis.[29] However, these studies may not be relevant to the Periana-Catalytica system as reactions were carried out at lower temperatures, in relatively weak nonoxidizing acids, and with model ligated Pt complexes that did not show CH activation of CH_4.

As shown in Scheme 5, if catalysis proceeds only by Pathway D, analogous to the treatment for Pathway B, kinetic analysis would predict the molar ratio of the D isotopologues of methane to methanol, $[(\text{mol } CH_nD_{4-n}])/(\text{mol } CH_mD_{3-m}X)]_{CAT}$ and would give $k_{-1}/(k_{-6}[X_2Pt^{IV}\text{-}X] + k_2[D_2SO_4])$ assuming that both steps k_2 and k_4 proceed at similar rates. Direct Pt^{II}-Me oxidation (k_2) is included in this analysis since no data have been obtained to rule out the involvement of this step for formation of product. Our analysis was focused on determining if Pathway A was the only pathway operating, and since Pathway C only includes the additional

Scheme 5. Kinetic Analysis of the Pathway D

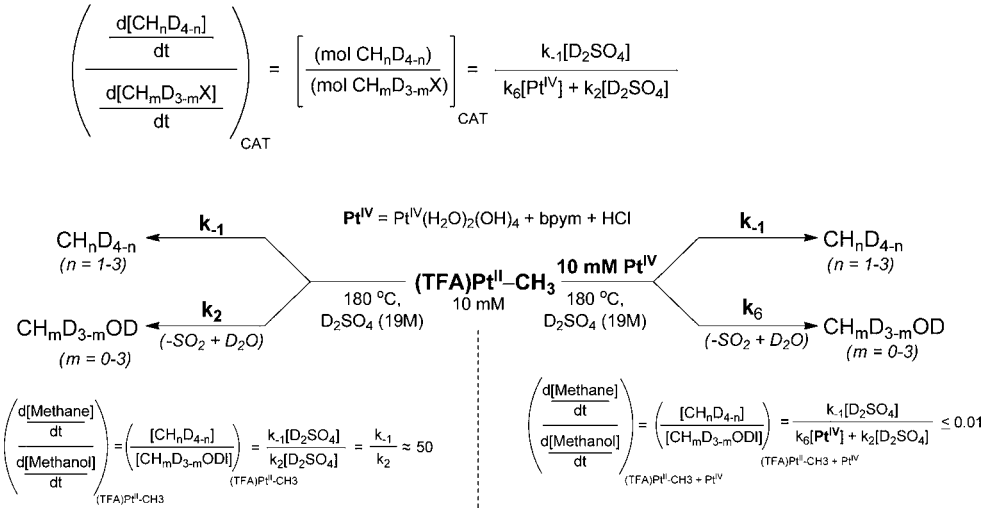

step k_2, product formation by both pathways cannot be ruled out. However, the focus of those analyses were on the basis for catalyst stability not product formation.

To examine whether Pathway D is the basis for catalysis, stoichiometric reactions of the independently synthesized complex, **(TFA)Pt^{II}-CH$_3$**, were examined as a model of **Pt^{II}-CH$_3$** and the molar ratio of (mol CH_nD_{4-n}/mol $CH_mD_{3-m}X$) obtained and compared to (mol CH_nD_{4-n}/mol $CH_mD_{3-m}X)_{CAT}$. The stoichiometric reactions examined are summarized in Scheme 5. To model Pathway D and the possibility for steps k_2 and k_6, the reactions were carried out in the absence and presence of a model of **X$_2$Pt^{IV}-X** (Table 1, entries 3 and 4, respectively). Attempts at using $(bpym)PtCl_4$ as a model of **X$_2$Pt^{IV}-X** were complicated by the instability of this complex in concentrated H_2SO_4. Consequently, a mixture of $Pt^{IV}(OH)_4(H_2O)_2$, bpym, and HCl (**Pt^{IV}** in Scheme 5) was used as a model of **X$_2$Pt^{IV}-X**.[30] As noted above, that mixture was found to be just as effective as **Pt^{II}-X** for catalyzing methane conversion. Assuming that **TFA-Pt^{II}-CH$_3$** reacts as expected for **Pt^{II}-CH$_3$** in Pathway D, the expected stoichiometric reactions are summarized in Scheme 5. As can be seen, if the reactions of **TFA-Pt^{II}-CH$_3$** are carried out in the absence of the **X$_2$Pt^{IV}-X** model (**Pt^{IV}**), then the molar ratio of products, $[(\text{mol } CH_nD_{4-n}])/(\text{mol } CH_mD_{3-m}X)]_{(TFA)Pt(II)-CH_3}$, should give k_{-1}/k_2. Step k_6 with **X$_2$Pt^{IV}X** should not take place assuming that under these conditions, step k_4 is not competitive with these steps. However, it is possible that rapid protonolysis of **TFA-Pt^{II}-CH$_3$** to generate **Pt^{II}**, followed by fast oxidation could generate **X$_2$Pt^{IV}X** that could complicate analysis. In the case of reaction of **TFA-Pt^{II}-CH$_3$** with **X$_2$Pt^{IV}X**, the molar ratio of products, $[(\text{mol } CH_nD_{4-n}])/(\text{mol } CH_mD_{3-m}X)]_{Pt(II)-CH_3+Pt(IV)}$ should be $k_{-1}/(k_6[X_2Pt^{IV}\text{-}X] + k_2(D_2SO_4))$. As for studies of Pathway B, the key hypothesis is that similarities between $[(\text{mol } CH_nD_{4-n}])/(\text{mol } CH_mD_{3-m}X)]_{CAT}$, $[(\text{mol } CH_nD_{4-n}])/(\text{mol } CH_mD_{3-m}X)]_{(TFA)Pt(II)-CH_3}$ and $[(\text{mol } CH_nD_{4-n}])/(\text{mol } CH_mD_{3-m}X)]_{(TFA)Pt(II)-CH_3+Pt(IV)}$ obtained from the stoichiometric reactions of the **(TFA)Pt^{II}-CH$_3$** model complex with and without **X$_2$Pt^{IV}X** would support the proposed mechanism while a poor match would rule against.

The stoichiometric reactions were carried out by injecting a 0.52 M solution of **TFA-Pt^{II}-CH$_3$** in DMSO into a glass vial containing a stirred solution of concentrated D_2SO_4 at 180 °C under argon. DMSO was used as the solvent as *in situ* studies by NMR showed **TFA-Pt^{II}-CH$_3$** was stable at RT for >30 min in this solvent. Immediately, upon injection, the reaction vial was removed and allowed to cool to RT, and the gas and liquid phases analyzed by GC-MS and ^{1}H NMR. The results (entry 3, Table 1) show that stoichiometric reaction of **TFA-Pt^{II}-CH$_3$** yielded CH_4 as essentially the only product, and only traces of CH_3X were detected with $[(\text{mol } CH_nD_{4-n})/(\text{mol } CH_mD_{3-m}X)]_{(TFA)Pt(II)-CH_3} \approx 50$ (within detection limits). As shown in Scheme 5, this suggests that the k_{-1} is faster than the k_2 step ($k_{-1} \approx 50k_2$). Importantly, while this ratio of products does not exactly match $[(\text{mol } CH_nD_{4-n}])/(\text{mol } CH_mD_{3-m}X)]_{CAT}$ obtained from catalysis, ~20, Table 1, entry 2, this ratio is a much better match than that from the stoichiometric reaction of **(TFA)(X)-Pt^{IV}-CH$_3$**, (<0.01), Table 1, entry 2. This could provide support for step k_1 in Pathway D, CH activation by **Pt^{II}-X** to give **Pt^{II}-CH$_3$**. This is also supported by theoretical studies that show the calculated activation barrier for CH activation from **Pt^{II}-X** of ~31 kcal/mol is lower than that obtained from experiment, ~33 kcal/mol. This contrasts with the substantially higher calculated barrier for CH activation with Pt^{IV} of ~41 kcal/mol.

As noted above, given the relatively fast rate of oxidation of **Pt^{II}-X** to **X$_2$Pt^{IV}X** in the absence of methane and the low expected concentration of **Pt^{II}-CH$_3$**, the k_6 step must be extraordinarily fast to be the basis for the stability of the system. To examine the feasibility of the k_6 step, the stoichiometric reaction of **TFA-Pt^{II}-CH$_3$** in concentrated D_2SO_4 at 180 °C was examined under the same conditions as before but with 1 equiv of **X$_2$Pt^{IV}-X** (added as a 1:1:1 mixture of $Pt^{IV}(OH)_4(H_2O)_2$, bpym, and HCl) added to the D_2SO_4 solvent prior to reaction. Remarkably, as shown in Table 1, entry 4, this reaction gave almost no CH_4 and only CH_3X with $([CH_nD_{4-n}])/([CH_mD_{3-m}X])_{(TFA)Pt(II)-CH_3+Pt(IV)} = <0.01$ (within detection limits). This is remarkable and shows that 10 mM **Pt^{II}-CH$_3$** (final concentration) is oxidized by 1 equiv **(TFA)XPt^{IV}-X** (10 mM), step k_6, at a rate significantly faster than both protonolysis, k_{-1}, and oxidation, k_2, by the reaction solvent, concentrated D_2SO_4 at 180 °C! As shown in Scheme 5, using a value of 19 M for the concentration of D_2SO_4, 10 mM for the concentration of **X$_2$Pt^{IV}X**, we estimate that k_6 is 10^5 times larger than k_{-1} and 10^7 larger than k_2.

dx.doi.org/10.1021/ja404895z | J. Am. Chem. Soc. 2013, 135, 14644−14658

These results make an important, testable prediction. The high rate of step k_6, relative to k_2 or k_{-1} would suggest that carrying out the actual catalytic reaction at low TON with added $\mathbf{X_2Pt^{IV}}$-X prior to reaction would result in a ratio of products, $([CH_nD_{4-n}])/([CH_mD_{3-m}D])_{CAT+Pt(IV)}$, that should be the same or very similar to the ratio of products from the stoichiometric reaction of $\mathbf{X_2Pt^{IV}}$-$\mathbf{CH_3}$, $([CH_nD_{4-n}])/([CH_mD_{3-m}D])_{(TFA)Pt(IV)\text{-}CH_3}$ (<0.01) used to examine Pathway B. In effect, under catalytic conditions added $\mathbf{X_2Pt^{IV}X}$ should trap almost all the $\mathbf{Pt^{II}}$-$\mathbf{CH_3}$ generated from CH activation with $\mathbf{Pt^{II}}$-X to generate primarily $CH_mD_{3-m}X$ and little CH_nD_{4-n}. In this reaction, it is critical that short reaction times and lower temperatures and pressures of CH_4 are utilized to ensure that the amount of CH_3X that would be generated by the catalytic oxidation of CH_4 with H_2SO_4 in the absence of $\mathbf{X_2Pt^{IV}}$-X is small relative to the amount of added $\mathbf{X_2Pt^{IV}}$-X prior to the catalytic reaction.

To test this prediction, the catalytic reaction was carried out at 150 °C and 25 psig of CH_4. Under these conditions, in the absence of an added model of $\mathbf{X_2Pt^{IV}}$-X, the amount of CH_3X generated by catalytic oxidation of CH_4 by H_2SO_4 after 30 min is low (TON <0.1, less than limits of detection), and the extent of H/D exchange with CH_4 is greater (>250%, TON = 2.5). Remarkably, repeating the reaction with 3 equiv of the 1:1:1 mixture of $Pt^{IV}(OH)_4(H_2O)_2$, bpym, and HCl as a model of $\mathbf{X_2Pt^{IV}}$-X led to stoichiometric amounts of CH_3X relative to the added $\mathbf{X_2Pt^{IV}}$-X model and very little H/D exchange. Table 1, entry 5, $(\sum[CH_nD_{4-n}])/([CH_mD_{3-m}X])_{CAT+Pt(IV)} < 0.01$ (within experimental error). Taken together, these results provide strong support for Pathway D as the basis for the high stability of the system. This type of reaction mechanism where the higher oxidation state of the catalyst is off-cycle and is brought back into the catalytic cycle by reaction with another intermediate can be considered to be a catalytic "self-repair" mechanism.

Additional evidence for CH activation by $\mathbf{Pt^{II}}$-X may also be obtained by comparison of the ratio of isotopologues CH_nD_{4-n} (n = 1−4) generated from the rapid, stoichiometric reaction of $\mathbf{TFA\text{-}Pt^{II}\text{-}CH_3}$ and the actual catalytic system. Figure 4 shows

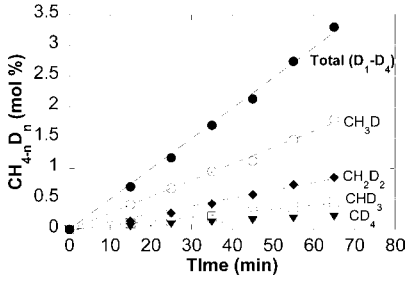

Figure 4. Time-dependent plot of mol % of the CH_4 isotopologues. CH_nD_{4-n} results from reaction between D_2SO_4 and CH_4 catalyzed by $(bpym)PtCl_2$.

the mol % of the various CH_4 isotopologues generated from the catalytic reaction as a function of time. Remarkably, these data show that even at short reaction times and low conversion of CH_4 (<5%), the various isotopologues are generated simultaneously (i.e., $CH_4 \rightarrow CH_nD_{4-n}$, with n = 1 − 3 all observed) rather than sequentially ($CH_4 \rightarrow CH_3D \rightarrow CH_2D_2$, etc.). In a sequential reaction, at low conversion of CH_4, assuming no large, inverse kinetic isotope effect, the primary product would be CH_3D without any of the more substituted isotopologues. Significantly, GC-MS analysis of the gas phase from the stoichiometric reaction of $\mathbf{Pt^{II}}$-$\mathbf{CH_3}$ with D_2SO_4 at 180 °C also shows that all the isotopologues of CH_nD_{4-n} (n = 0−3) are formed (see SI). This distribution is remarkable since the stoichiometric reaction is stopped immediately upon mixing and is irreversible (the resulting concentration of CH_4 is very low and the reaction times very short). The similarity of simultaneous formation of the isotopologues, CH_nD_{4-n}, n = 1−3) from the catalytic system and stoichiometric reaction further supports step k_1 in Pathway D, the CH activation by $\mathbf{Pt^{II}}$-X to give $\mathbf{Pt^{II}}$-$\mathbf{CH_3}$. Consistent with these results, DFT studies show that the formation of the various isotopologues is due to reversible protonolysis of $\mathbf{Pt^{II}}$-$\mathbf{CH_3}$ to yield the corresponding CH_4 complex $[\mathbf{Pt^{II}}\text{-}(\mathbf{CH_4})]^+$ before loss of CH_4 and generation of $\mathbf{Pt^{II}}$-X.[29]

DFT Calculations. These experiments show that the activation barrier for the k_6 step in Pathway D must be lower than the protonolysis of $\mathbf{Pt^{II}}$-$\mathbf{CH_3}$, step k_{-1} as well as for oxidation of $\mathbf{Pt^{II}}$-$\mathbf{CH_3}$ to generate $\mathbf{X_2Pt^{IV}}$-$\mathbf{CH_3}$, step k_2, by the reaction solvent H_2SO_4 at 180 °C! The high concentration of H_2SO_4 (19 M) and a maximum concentration of 10 mM $\mathbf{X_2Pt^{IV}X}$ would suggest that the barrier for step k_6 could be <10 kcal/mol. To examine this reaction more closely, we examined these pathways via DFT calculations. This type of bimolecular reaction between $\mathbf{Pt^{II}}$-$\mathbf{CH_3}$ and $\mathbf{X_2Pt^{IV}}$-X to generate $\mathbf{X_2Pt^{IV}}$-$\mathbf{CH_3}$ and $\mathbf{Pt^{II}}$-X could proceed via electron or methyl transfer. However, as a result of the studies of the Shilov system showing that reactions with model complexes proceed via an electron transfer,[6c] we did not examine the transition states for methyl transfer. On the basis of the classical self-exchange studies involving inner-sphere electron transfer (ISET) between four-coordinate, square planar $[Cl_4Pt^{II}]^{2-}$ and octahedral $[Cl_6Pt^{IV}]^{2-}$ salts,[6] the reaction of $\mathbf{Pt^{II}}$-$\mathbf{CH_3}$ with $\mathbf{X_2Pt^{IV}}$-X could proceed as shown in Scheme 6 via nucleophilic activation of $\mathbf{Pt^{II}}$-$\mathbf{CH_3}$. In

Scheme 6. Postulated Mechanism for ISET between $\mathbf{Pt^{II}}$-$\mathbf{CH_3}$ and $\mathbf{X_2Pt^{IV}}$-X by Nucleophilic or Electrophilic Activation

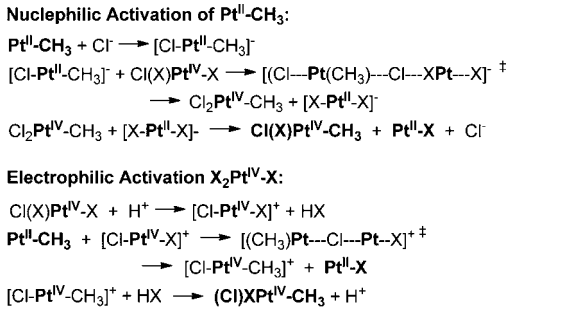

this case, the $\mathbf{Pt^{II}}$-$\mathbf{CH_3}$ is activated by addition of Cl^-, the strongest potential nucleophile in the catalytic system, to generate a five-coordinate, $[Cl\text{-}\mathbf{Pt^{II}}\text{-}CH_3]^-$ intermediate with a more nucleophilic Pt-centered lone pair. This activated species can attack the Cl of $Cl(X)\mathbf{Pt^{IV}}$-X to generate $\mathbf{Cl_2Pt^{IV}}$-$\mathbf{CH_3}$ by "displacing" $[X\text{-}\mathbf{Pt^{II}}\text{-}X]^-$ that subsequently losses Cl^- to generate $\mathbf{Pt^{II}}$-X, Scheme 6. This ISET could also be seen as a formal Cl^+ transfer.

Since it would seem that such a nucleophilic activation of $\mathbf{Pt^{II}}$-$\mathbf{CH_3}$ may not be plausible in a strongly acidic media, we also considered the complementary possibility that the reaction could be facilitated by electrophilic activation of the $\mathbf{X_2Pt^{IV}}$-X species by the concentrated H_2SO_4 solvent. In this case, reaction of $\mathbf{X_2Pt^{IV}}$-X with H^+ leads to loss of HX and generates

dx.doi.org/10.1021/ja404895z | J. Am. Chem. Soc. 2013, 135, 14644−14658

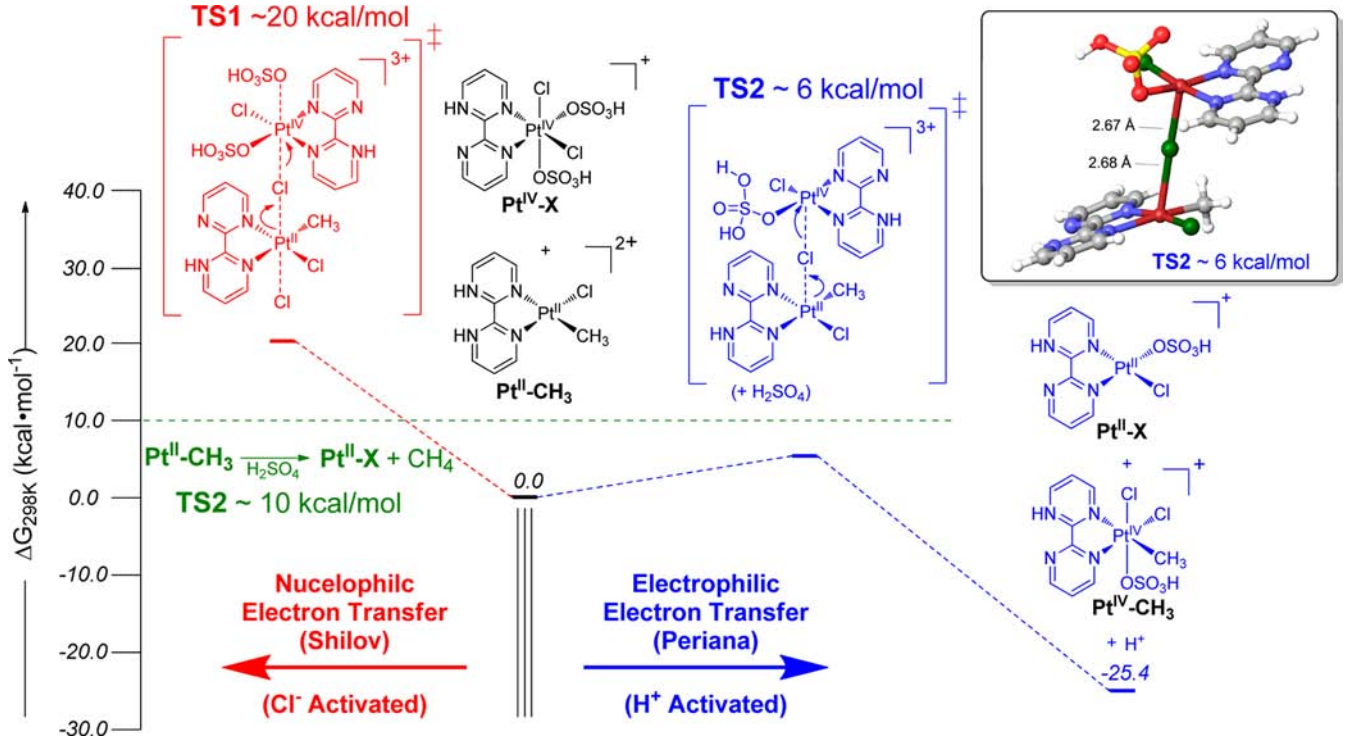

Figure 5. Calculated transition states for the ISET between Pt^{II}-CH_3 to the X_2Pt^{IV}-X by nucleophilic (Left) and electrophilic (right) activation.

a more electrophilic five-coordinate, cationic Pt^{IV} species, [Cl-Pt^{IV}-X]$^+$. In this species, the -Cl attached to the five-coordinate Pt center would be electrophilically activated to react nucleophilically with the lone pair of the unactivated Pt^{II}-CH_3 to generate Pt^{II}-X and [Cl-Pt^{IV}-CH_3]$^+$ that can subsequently react with HX to generate X_2Pt^{IV}-CH_3 and regenerate the H^+.

As can be seen in Figure 5, DFT calculations show that the pathway involving nucleophilic activation of Pt^{II}-CH_3 with Cl^- **TS1** proceeds with a ~20 kcal/mol barrier. The previously reported[31] barrier for protonolysis of Pt^{II}-CH_3 (transition state not shown, see SI) by concentrated H_2SO_4 to generate CH_4 was calculated to be ~10 kcal/mol, **TS2**. Consequently, since the experimental data, Table 1, entry 4, show that the k_6 step is faster than the protonolysis step, k_{-1}, it is unlikely the step k_6 between Pt^{II}-CH_3 with X_2Pt^{IV}-X proceeds via **TS1** involving nucleophilic activation of Pt^{II}-CH_3. Remarkably, consistent with the experimental observations, the reaction of Pt^{II}-CH_3 with the five-coordinate species resulting from electrophilic activation of X_2Pt^{IV}-X with H_2SO_4 shows a transition of state, **TS2**, of ~6 kcal/mol. This result provides strong additional support for the k_6 step and Pathway D as the basis for the catalysts stability.

Mechanism for Product Formation. As noted earlier, the pathways that account for product stability and product formation need not be the same. Thus, while Pathway D can account for the high stability of the system, it is possible that Pathways D and A (involving direct oxidation of Pt^{II}-CH_3 with H_2SO_4 to generate X_2Pt^{IV}-CH_3, the k_2 step) are competitive and that both contribute to product formation. The observation that the reaction of Pt^{II}-CH_3 with 1 equiv of X_2Pt^{IV}-X generates almost exclusively CH_3X, entry 2, Table 1, could suggest that Pathway D may be the pathway that accounts for both the high stability of the system and the product generation. However, if the steady-state concentration of X_2Pt^{IV}-X is very low, then step k_2 could be competitive with step k_6 and Pathways A and D could be competitive. Since the k_2 step in Pathway A could not be examined due to rapid protonolysis of the (TFA)-Pt^{II}-CH_3 model complex, the feasibility and energetics for the direct oxidation of Pt^{II}-CH_3 with concentrated H_2SO_4 (containing SO_3) to generate X_2Pt^{IV}-CH_3 were investigated using DFT.

A composite energy diagram of the two pathways, D and A, are summarized in Figures 6 and 7, respectively. These pathways were based on the lowest energy species identified. However, there could be other lower energy pathways. It should be noted that the lowest energy pathway identified for the direct oxidation of Pt^{II}-CH_3 involves the reaction of Pt^{II}-X with H_2SO_4/SO_3 to generate a Pt^{II}-SO_3H adduct with a Pt−S bond. This is similar to the species identified by Ziegler in studies of this reaction.[16] Pathways involving electron transfer via O or Cl^- bridges between Pt and S of H_2SO_4 were significantly higher in energy. Assuming the presence or a small energetic cost for formation of SO_3 under the reaction conditions, an important conclusion from the DFT studies is that the rates of Pathways A and D could be comparable. This would suggest that while Pathway D is essential to the catalyst stability, both Pathways A and D could contribute to product generation. However, since the catalysis can be carried out between 90−98%, where the concentration of free SO_3 is low, it is possible that Pathway A is not accessible and that Pathway D accounts for both the stability and product formation.

Perhaps the most important conclusion from this study is that the rate-determining step in Pathway D is k_4, the oxidation of Pt^{II}-X to X_2Pt^{IV}-X. This would suggest that increasing the rate of this step could increase the rate of catalysis in the Periana-Catalytica system. Since k_1, k_6, and k_3 have much lower barriers than k_4, it is possible that significant increases in rate could be possible without causing the system to deactivate. This is important to recognize since it is opposite of the accepted view that oxidation of the reduced state of a catalyst, to the

dx.doi.org/10.1021/ja404895z | J. Am. Chem. Soc. 2013, 135, 14644−14658

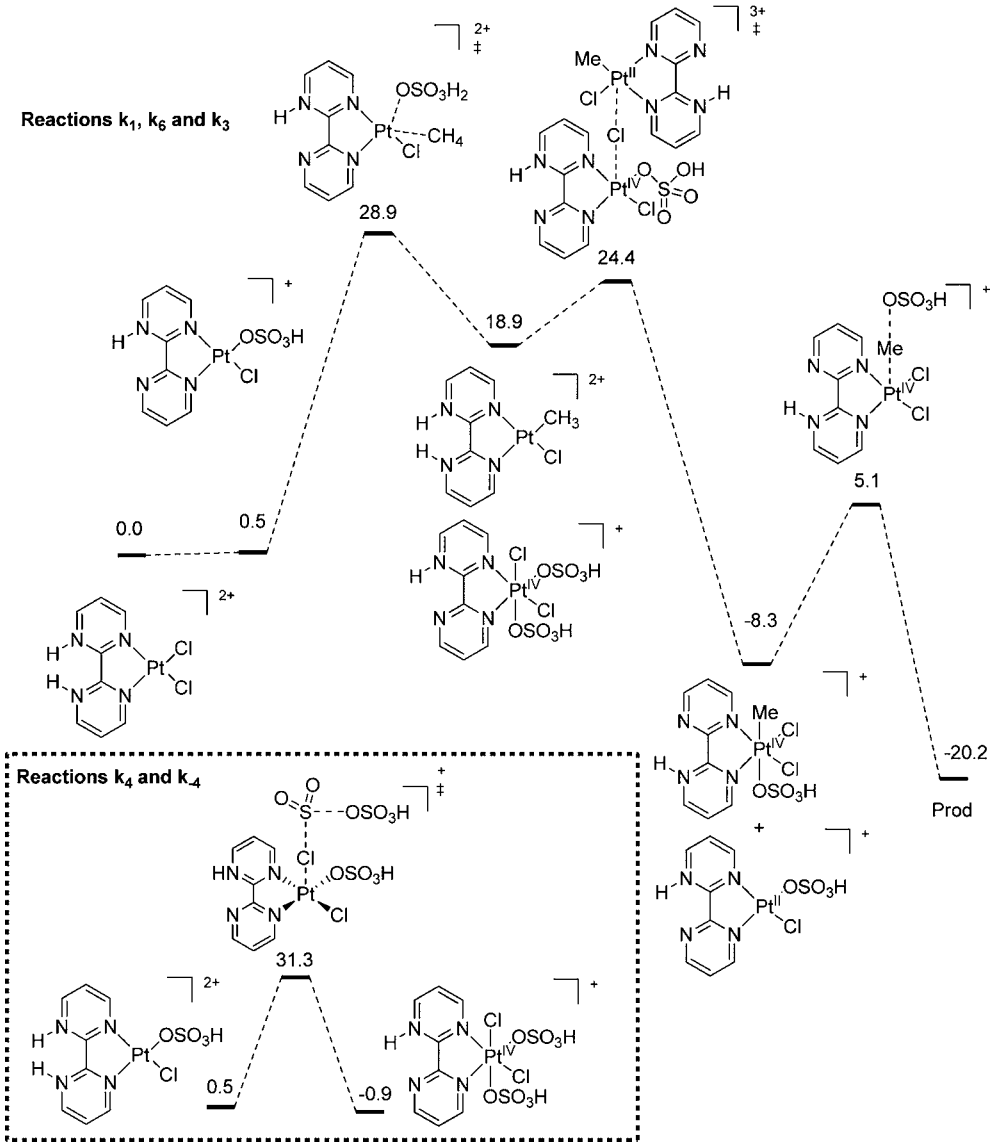

Figure 6. Energy diagram from DFT of Pathway D.

more stable higher oxidation state that is active for CH activation, must be suppressed to prevent catalyst deactivation. We have begun to study methods of increasing, rather than suppressing, the rate of this k_4 oxidation reaction in our laboratory with the objective of increasing the rate of catalysis. We would like to emphasize that other parallel mechanisms for oxidation of **Pt^{II}-X** are also possible. However, no other mechanism with a low barrier was located. The mechanism proposed by Ziegler via S−O oxidative addition was calculated to have a barrier of 44.9 kcal mol^{-1}, in agreement with the previous study.[16]

CONCLUSION

Studies of the highly stable, Periana-Catalytica (bpym)$PtCl_2$ catalyst for the oxidation of methane with concentrated sulfuric acid at 200 °C to methanol have been shown to operate by a more complex mechanism than previously considered. Mechanistic studies show that, consistent with the original proposals, Pt^{IV} is not active for reaction with methane and that the reaction proceeds by CH activation with a Pt^{II} species to generate Pt^{II}-CH_3. Significantly, in the absence of methane, the (bpym)$Pt^{II}Cl_2$ catalyst has been found to rapidly oxidize in concentrated H_2SO_4 at 200 °C to Pt^{IV}. Unexpectedly, contrary to the general teaching that the oxidation of the Pt^{II} to Pt^{IV} should be minimized in order to prevent catalyst deactivation, studies show that increasing the rate of this over oxidation of Pt^{II} can actually lead to stable systems with higher TOF. Detailed experimental and DFT calculations show that this result is because oxidation of Pt^{II} to Pt^{IV}, the rate determining step, and because there is a fast "self-repair" reaction between Pt^{IV} and Pt^{II}-CH_3 by an ISET mechanism with the barrier of ∼6 kcal/mol that regenerates the Pt^{II}.

These studies could be generalized to provide new considerations for the design of oxidation catalysts based on CH activation with a reduced species, LM^n, Scheme 2, that is thermodynamically unstable to oxidation to higher, oxidation states, $LM^{>n}$ that are inactive for reaction with the alkane. In such systems, to prevent rapid deactivation by catalyst "pooling" to $LM^{>n}$, it is generally accepted that the oxidation of LM^n to $LM^{>n}$ should be minimized and/or much slower than oxidation of LM^n-CH_3. However, since the oxidant must be present in large excess and LM^n-CH_3 is generally present at

dx.doi.org/10.1021/ja404895z | J. Am. Chem. Soc. 2013, 135, 14644−14658

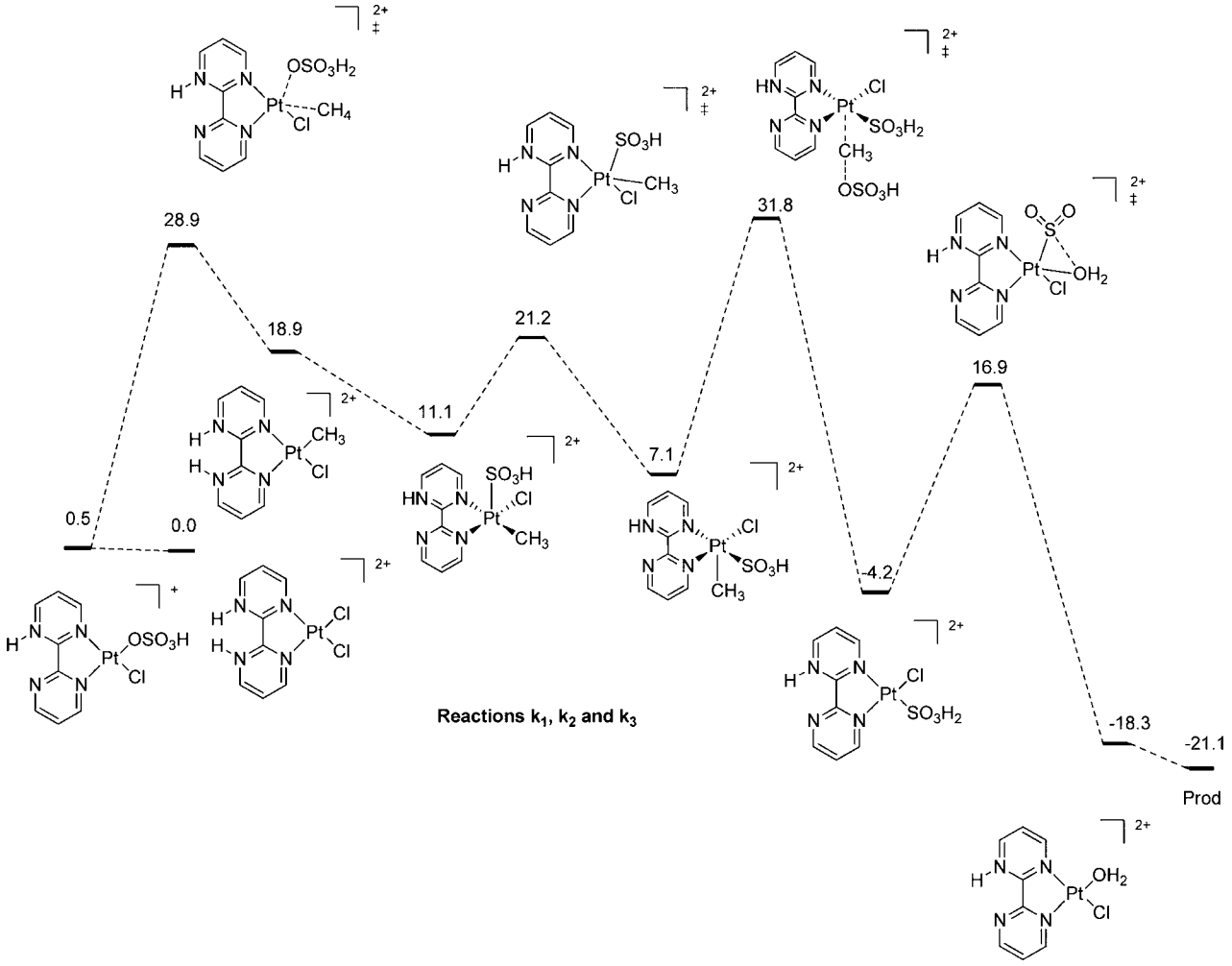

Figure 7. Energy diagram from DFT of Pathway A.[29]

very low concentrations relative to LM^n (since the thermodynamics of CH activation is typically >15 kcal/mol), it is unlikely[32] that this can be generally achieved. In any case, any finite and irreversible oxidation of LM^n required for reaction with the alkane to $LM^{>n}$ will ultimately lead to catalyst deactivation. To minimize or prevent deactivation in oxidizing media, these studies would suggest that it is critical to focus on the design of catalyst systems, with a "self-repair" mechanism, Scheme 7, involving the LM^n-CH_3 species (resulting from CH activation with LM^n) and $LM^{>n}$ that regenerates the LM^n species. Indeed, such a reaction could be more important than the generally accepted focus to minimize oxidation of LM^n since, if the rate of self-repair is comparable to the oxidation of LM^n, such catalyst systems can be indefinitely stable to deactivation by over oxidation.

Scheme 7. Generalized Mechanism for the Design of Efficient Oxidation Catalysts That Operate by CH activation with the Reduced Species, LM^n-X

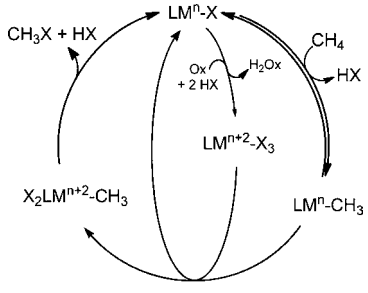

These studies also show that in addition to the "self-repair" mechanism based on ISET between the LM^n-CH_3 and LM^{n+2}-X_3, other strategies to avoid catalyst deactivation are to ensure that: (A) oxidation of the lower, oxidation state, LM^n required for reaction with the alkane to $LM^{>n}$ is reversible, (B) the highest thermodynamically accessible oxidation state, $LM^{>n}$, is the species most active for CH activation, or (C) there is fast alkyl transfer between LM^n-CH_3 and LM^{n+2}-X_3 to generate LM^{n+2}-CH_3. These principles may help to guide the design of catalysts for the oxidation of unactivated hydrocarbons based the CH activation reaction.

EXPERIMENTAL SECTION

General Procedures. Unless otherwise noted, all reactions were carried out under an inert atmosphere of nitrogen or argon utilizing standard Schlenk glassware techniques or a Vacuum Atmospheres drybox. Elemental analyses were carried out by Desert Analytics Laboratory, Tucson, AZ. ^{1}H, ^{13}C, and ^{19}F NMR spectra were collected using Bruker AC-250 (^{1}H at 250.134 MHz and ^{13}C at 62.902 MHz), AM-360 (^{1}H at 360.138 MHz and ^{13}C at 90.566 MHz), and Varian Mercury 400 spectrometers (^{1}H at 400.151 MHz and ^{13}C at 100.631 MHz). The spectra were referenced to residual solvent protons or a known chemical shift standard, and chemical shifts are reported in

dx.doi.org/10.1021/ja404895z | J. Am. Chem. Soc. 2013, 135, 14644−14658

parts per million downfield of tetramethylsilane. All coupling constants are reported in Hertz. NMR experiments requiring air-free manipulations were carried out in Wilmad NMR tubes fitted with J. Young Teflon vacuum/pressure valves. Liquid and gas phases of reaction products were analyzed on a Shimadzu QP-5000 GC-MS instrument. Gas phases were analyzed using a J&W Scientific GasPro capillary column (30 m × 0.32 mm ID), liquid phase on J&W Scientific DS-5 ms capillary column (30 m × 0.32 mm ID). Unless otherwise noted, reagent grade chemicals were purchased from commercial suppliers and used without further purification. Hydrocarbon solvents, ether, and THF were distilled from sodium/benzophenone under argon; inhibitor-free dry dichloromethane was obtained via standard procedures and finally purified by careful distillation from CaH_2 immediately prior to use. Deuterated solvents for NMR experiments were purified by identical procedures. SO_2 was distilled from P_2O_5 directly into an NMR tube immediately prior to use except during reactions on larger scale (described separately below).

Catalytic CH_4 oxidation experiments were carried out as described in the original procedures with a 25 mL Hastaloy C, Autoclave Engineers' Mini-Reactor equipped with a glass vial and an externally stirred DespersiMax stirrer.[13] For NMR analysis, a known amount of acetic acid was added to an aliquot of the reaction solution as an internal standard. If required, HCl was added using finely ground solid KCl, as KCl reacts with hot, concentrated H_2SO_4 to instantly generate 1 equiv of HCl. The specified amount of solid KCl was added to a thin-walled NMR tube that was cut to ∼2 in. Before the reactor was sealed, the tube was placed such that the KCl was not in contact with the concentrated H_2SO_4. Control experiments shown that upon stirring, the vial breaks, and the KCl reacts to generate HCl. Control experiments showed that small amounts of $KHSO_4$ generated in this reaction, typically 1−2 equiv relative to catalyst, had no effect on the catalytic reaction. Methyl bisulfate (and any free CH_3OH) was determined from the ratio of the ^1H NMR methyl resonances of methyl bisulfate (3.4 ppm) to acetic acid (2.02 ppm). The methyl products were also quantified by HPLC analysis of the liquid phase. Known volume aliquots of reaction solution were first hydrolyzed by the addition of 3 parts water to 1 part crude reaction solution and heated to 90 °C for 4 h in a sealed vial. The hydrolyzed solution was analyzed using a HP 1050 HPLC equipped with a HPX-87H column (Bio-Rad) and a refractive index detector. The eluent was 0.1 vol % sulfuric acid in water. CH_3OH eluted at 16.2 min. The gas phase (CH_4, CO_2, and CH_3Cl) and liquid phase (CH_3OSO_3H and CH_3OH) analyses allowed >90% mass balance on CH_4.

Compounds. *(bpym)PtCl$_2$.* Synthesis of this compound was reported previously.[33] However, it was found that the following simple method was more efficient. In a 30 mL vial, 0.085 g of 2,2′-bipyrimidine was combined with 0.222 g K_2PtCl_4 in 15 mL H_2O at RT in air. After stirring overnight, an orange precipitate formed which was filtered off, washed with acetone (4 × 50 mL), followed by ether (4 × 100 mL), and then dried *in vacuo* to give a yield of 99%. ^1H NMR (500.1 MHz, DMSO-d_6): δ 8.00 (dd, 2 H, bpym $H_{5/5'}$), 9.35 (dd, 2 H, bpym $H_{4/4'}$), 9.68 (dd, 2 H, bpym $H_{6/6'}$). $^{13}C\{1H\}$ NMR (125.8 MHz, DMSO-d_6): δ 124.4 (s, bpym $C_{5/5'}$), 154.6 (s, bpym $C_{4/4'}$), 159.7 (s, bpym $C_{6/6'}$), 162.0 (s, bpym $C_{2/2'}$). Anal. calcd for $C_8H_6Cl_2N_4Pt$ (M_r = 424.15): C, 22.65; H, 1.43; N 13.21; Cl, 16.72. Found: C, 23.13; H, 1.19; N 13.33; Cl, 16.74.

Pt(bpym)Cl$_4$. In a flask, 0.9 g K_2PtCl_6 was combined with 0.3 g 2,2′-bipyrimidine in 35 mL H_2O and heated to 95 °C to achieve complete dissolution of the components. The solution was stirred for 1 h during which time an orange precipitate formed (which was determined to be the desired product contaminated with $Pt(bpym)Cl_2$). After that, Cl_2 gas was bubbled through the resulting suspension for 10 min, turning the color of the precipitate to bright lemon. The mixture was cooled to 0 °C, and the precipitate was filtered off, washed twice with chilled H_2O, and dried *in vacuo* to give an 85% yield. ^1H NMR (500.1 MHz, DMSO-d_6): δ 8.36 (dd, 2 H, bpym $H_{5/5'}$), 9.57 (dd, 2 H, bpym $H_{4/4'}$), 9.79 (dd+dd, 2 H, $^3J_{Pt-H}$ = 25.7 Hz, bpym $H_{6/6'}$). $^{13}C\{1H\}$ NMR (90.6 MHz, DMSO-d_6): δ 127.4 (s+d, $^3J_{Pt-C}$ = 21.4 Hz, bpym $C_{5/5'}$), 154.9 (s+d, $^4J_{Pt-C}$ = 11.1 Hz, bpym $C_{6/6'}$), 158.3 (s+d, $^2J_{Pt-C}$ = 16.7 Hz, bpym $C_{2/2'}$), 163.9 (s, bpym $C_{4/4'}$). Anal. calcd for $C_8H_6Cl_4N_4Pt$ (M_r = 495.05): C, 19.41; H, 1.22; N 11.32; Cl, 28.65. Found: C, 19.44; H, 1.29; N 11.01; Cl 28.76. X-ray quality yellow needles of were grown by vapor diffusion of diethyl ether into a dimethylformamide solution of $Pt(bpym)Cl_4$.

[Pt(CH$_3$)$_2$(μ-S(CH$_3$)$_2$]$_2$:[34] An ether solution of CH_3Li (2.3 mL of 1.4 M solution) was added dropwise to a chilled (0 °C) suspension of 0.58 g of $[Pt(Cl)_2(\mu\text{-}S(CH_3)_2]_2$[35] (mixture of *cis*- and *trans*-) in 25 mL of ether. After stirring at 0 °C for 15 min (or until the reaction mixture turns from yellow to white), the reaction mixture was warmed slowly to RT and hydrolyzed with 5 mL of a saturated NH_4Cl solution. The ether layer was separated, dried, and carefully evaporated *in vacuo* to give the desired product in 97% yield. ^1H NMR (500.1 MHz, $CDCl_3$): δ 0.47 (s+d, w/Pt satellites, 12 H, $^2J_{Pt-H}$ = 85.5 Hz, $-CH_3$), 1.58 (t, 12 H, $-CH_2CH_3$), 3.02 (q, 8 H, $-CH_2CH_3$). $^{13}C\{1H\}$ NMR (125.8 MHz, $CDCl_3$): δ −6.4 (s+d, $^1J_{Pt-C}$ = 780.2 Hz, -CH_3), 12.3 ((s+d, $^3J_{Pt-C}$ = 15.5 Hz, $-CH_3CH_3$), 29.6 (s+d, $^2J_{Pt-C}$ = 38.2 Hz, -CH_3CH_3). Anal. calcd for $C_{12}H_{32}Pt_2S_2$ (M_r = 630.67): C, 22.85; H, 5.11. Found: C, 22.85; H, 4.93.

Pt(bpym)(CH$_3$)$_2$. A variation of the previously reported method for preparation of $Pt(bpym)Cl_2$ was used.[36] A solution of 0.33 g of $[Pt(CH_3)_2(\mu\text{-}S(CH_3)_2]_2$ in 18 mL CH_2Cl_2 was quickly added to a solution of 0.828 g 2,2′-bipyrimidine (5 equiv per Pt) in 12 mL CH_2Cl_2 in air. After stirring for 1 h at RT, the solution turned dark red. Small amount of black-red precipitate was formed, which was filtered off, and the obtained clear dark-red filtrate was evaporated to dryness. Recrystallization of this residue from CH_3OH afforded pure product as bright-red microcrystalline powder in 75% yield. ^1H NMR (500.1 MHz, CD_2Cl_2): δ 1.04 (s+d, 6 H, $^2J_{Pt-H}$ = 87.3 Hz, $-CH_3$), 7.64 (dd, 2 H, bpym $H_{5/5'}$), 9.28 (dd, 2 H, bpym $H_{4/4'}$), 9.40 (dd+dd, 2 H, $^3J_{Pt-H}$ = 23.0 Hz, bpym $H_{6/6'}$). $^{13}C\{1H\}$ NMR (125.8 MHz, CD_2Cl_2): δ −16.9 (s+d, $^1J_{Pt-C}$ = 827.3 Hz, -CH_3), 124.6 (s+d, $^3J_{Pt-C}$ = 15.5 Hz, bpym $C_{5/5'}$), 153.6 (s+d, $^2J_{Pt-C}$ = 29.4 Hz, bpym $C_{6/6'}$), 157.0 (s, bpym $C_{4/4'}$), 163.2 (s, bpym $C_{2/2'}$). Anal. calcd for $C_{10}H_{12}N_4Pt$ (M_r = 383.31): C, 31.33; H, 3.16; N, 14.62. Found: C, 31.52; H, 3.10; N, 14.53.

Pt(bpym)(CH$_3$)OCOCF$_3$: (TFA)-Pt^{II}−CH$_3$. HTFA was added to a solution of 80 mg (0.209 mmol) of $Pt(bpym)(CH_3)_2$ in 8 mL of CH_2Cl_2, 16 μL (0.209 mmol) at −78 °C. The red solution immediately turned black, and a suspension was formed. The reaction mixture was allowed to warm to RT. This was accompanied by gas evolution and dissolution of the suspension, giving an orange solution. After addition of 50 mL of hexanes, a bright-yellow solid precipitated was filtered off and dried *in vacuo* to give a 90% yield. ^1H NMR (360.1 MHz, CD_2Cl_2): δ 1.12 (s+d, 3 H, $^2J_{Pt-H}$ = 79.5 Hz, $-CH_3$), 7.60 (dd, 1 H, bpym $H_{5\text{ or }5'}$), 7.81 (dd, 1 H, bpym $H_{5\text{ or }5'}$), 8.93 (dd, 1 H, bpym $H_{4\text{ or }4'}$), 9.25 (dd, 1 H, bpym $H_{4\text{ or }4'}$), 9.29 (dd, 1 H, bpym $H_{6\text{ or }6'}$) 9.32 (dd+dd, 1 H, $^3J_{Pt-H}$ = 60.0 Hz, bpym $H_{6/6'}$). $^{13}C\{1H\}$ NMR (90.6 MHz, CD_2Cl_2): δ −13.5 (s+d, $^1J_{Pt-C}$ = 787.1 Hz, -CH_3), 115.8 (q, $-OCOCF_3$, $^1J_{C-F}$ = 290.2 Hz), 124.4 (s+d, $^3J_{Pt-C}$ = 48.3 Hz, bpym $C_{4/4'}$), 125.3 (s, bpym), 154.4 (s, bpym), 157.0 (s+d, $^4J_{Pt-C}$ = 42.8 Hz, bpym), 158.0 (s, bpym), 159.7 (s, bpym), 160.7 (s, bpym $C_{2/2'}$), 162.7 (q, -$OCOCF_3$, $^2J_{C-F}$ = 36.3 Hz), 164.2 (s, bpym $C_{2/2'}$). ^{19}F NMR (470.6 MHz, CD_2Cl_2): δ −74.6 (s, $-OCOCF_3$). Anal. calcd for $C_{11}H_9F_3N_4O_2Pt$ (M_r = 481.29): C, 27.45; H, 1.88; N 11.64. Found: C, 27.10; H, 2.12; N 11.55. X-ray quality orange needles of $Pt(bpym)(CH_3)(OCOCF_3)\cdot CH_2Cl_2$ were obtained by crystallization from dichloromethane.

Pt(bpym)(CH$_3$)(OCOCF$_3$)Cl$_2$. 50 mg (0.131 mmol) of $Pt(bpym)(CH_3)OCOCF_3$ was dissolved in 20 mL CH_2Cl_2 at −78 °C, and excess Cl_2 gas was added to the reaction flask. On stirring, the reaction mixture changed color from orange red to pale yellow, at which point stirring was stopped, and excess chlorine and solvent were removed *in vacuo* (10 mTorr) while still maintaining the reaction mixture at low temperature. A light-yellow solid was obtained, which was only stable in the solid state at temperatures below −30 °C in 95% yield. Solutions are stable at RT. Above this temperature, the solid quickly decomposes unless excess Cl_2 is present. The complex is soluble in DMSO and CH_2Cl_2. ^1H NMR (500.1 MHz, CD_2Cl_2): δ 3.05 (s+d, 3 H, $^2J_{Pt-H}$ = 68.2 Hz, $-CH_3$), 7.84 (dd, 1 H, bpym H_x), 7.92 (dd, 1 H,

dx.doi.org/10.1021/ja404895z | J. Am. Chem. Soc. 2013, 135, 14644−14658

bpym H_x), 8.87 (dd+dd, 1 H, $^2J_{Pt-H}$ = 35.7 Hz, bpym H_4), 9.20 (dd, 1 H, bpym H_x), 9.28 (dd, 1 H, bpym H_x), 9.56 (dd, 1 H, bpym H_x); coordinated CH_2Cl_2 molecule observed in DMSO: ^{1}H NMR (DMSO-d_6): δ 3.05 (s+d, 3 H, $^2J_{Pt-H}$ = 60.5 Hz, $-CH_3$), 5.76 (s, 1 H, 1/2 CH_2Cl_2), 8.18 (dd, 1 H, bpym H_x), 8.33 (dd, 1 H, bpym H_x), 9.32 (dd, 1 H, bpym H_x), 9.44 (dd+dd, 2 H, bpym H_x + bpym H_x), 9.55 (dd, 1 H, bpym H_x). ^{13}C{1H} NMR (125.8 MHz, CD_2Cl_2): δ 15.5 (s+d, $^2J_{Pt-C}$ = 465.7 Hz, -CH_3), 113.8 (q, $-OCOCF_3$, $^1J_{C-F}$ = 290.7 Hz), 125.5 (s+d, $^3J_{Pt-C}$ = 27.6 Hz, bpym $C_{4/4'}$), 125.9 (s, bpym), 155.1 (q, -$OCOCF_3$, $^2J_{C-F}$ = 41.3 Hz), 156.9 (s, bpym), 157.5 (s, bpym), 158.6 (s, bpym $C_{2/2'}$), 161.7 (s, bpym), 161.9 (s, bpym $C_{2/2'}$), 162.6 (s, bpym). ^{19}F NMR (470.6 MHz, CD_2Cl_2, C_6F_6 ref.): δ −77.0 (s, $-OCOCF_3$). Elemental analysis and NMR spectra consistent with the formula $Pt(bpym)(CH_3)(OCOCF_3)Cl_2{\cdot}0.5CH_2Cl_2$. Anal. calcd for $C_{11.5}H_{10}Cl_3F_3N_4O_2Pt$ (M_r = 594.67): C, 23.23; H, 1.69; N, 9.42. Found: C, 23.18; H, 1.68; N, 9.22.

Catalytic Reactions. *General Procedure for H/D Exchange.* Unless otherwise stated, a 25 mL Hastaloy C, Autoclave Engineers' Mini-Reactor equipped with a glass vial and an externally stirred DespersiMax stirrer was charged with 10 mL of a 5 mM solution containing $Pt(bpym)Cl_2$ dissolved in 98% D_2SO_4. The reactor was purged under CH_4 several times and pressurized to the final reaction pressure (typically 500 psig, unless otherwise noted). The reactor was then placed in a temperature-controlled jacket for the duration of the experiment. Upon completion of the reaction, the reaction was cooled to RT. Gas phase analysis was performed by venting a portion of the gas phase into a septum capped, evacuated vial. Liquid phase analysis was performed by ^{1}H or ^{13}C NMR using HOAc as an internal standard.

Analysis of H/D Exchange with CH_4 and D_2SO_4. The extent of H/D exchange was monitored by GC-MS. The percent deuterium incorporation into CH_4 was determined by deconvoluting the mass fragmentation pattern for CH_4 using an in-house developed Microsoft Excel program.[37] An important assumption built into the program is that there are no isotope effects on the fragmentation pattern of CH_4. The parent ion peak of CH_4 is relatively stable toward fragmentation and can be used to quantify the exchange reactions. The mass fragmentation pattern between 16 and 20 m/z was analyzed for each reaction and compared to control reactions not containing catalyst. The results obtained by this method are accurate within ±5% of deuterium incorporation or loss.

Reactions with Added SO_2. Reactions with added SO_2 on large scale were carried out as described in the original report[13] but with 200 psig of SO_2 prior to addition of CH_4, which was loaded at 700 psig (500 psig of CH_4). The SO_2 addition was accomplished by use of a 150 mL Hoke pressure vessel containing 25 mL of liquid SO_2 (this should be done in pressure vessel that is rated to a pressure of 1800 psig for safety and also containing a rupture disc) that is connected to the pressure reactor through high-pressure tubing utilizing a high-pressure valve. The vessel is heated to 100 °C (where the vapor pressure is ∼450 psig) with heating tape and gaseous SO_2 added to 200 psig. CH_4 was then fed from a high-pressure tank (>200 psig) to reach a final pressure of 700 psig.

Stoichiometric Reactions of Model Complexes. The stoichiometric reactions were carried out by directly injecting 0.1 mL of a 0.52 M solution of the model Pt−Me complex in DMSO all at once into a magnetically stirred 8 mL glass vial, equipped with a Teflon seal containing 5 mL of concentrated H_2SO_4 or D_2SO_4 heated to a 180 °C with an oil bath. When X_2Pt^{IV}-X was required, $Pt^{IV}(OH)_4(H_2O)_2$ (15.5 mg, 51.9 μmol, 1 equiv), bpym (8.2 mg, 51.9 μmol, 1 equiv), and 12 M HCl (8.7 μL, 104.9 μmol, 2 equiv) were added to the H_2SO_4 or D_2SO_4 before the reaction, as specified in the discussion. Upon addition, the vial was immediately removed and cooled in an ice bath. 2.5 mL of ethane and 5 μL of AcOH were added as gas and liquid standards, respectively. The liquid and gas phases were then sampled and analyzed as described above.

Determination of SO_2 Generated from Pt^{II}-X. The reactions were carried out in duplicate by sealing two 5 mL portions of a 10 mM solution of $Pt(bpym)Cl_2$ in 98% H_2SO_4, placed into two separate 8 mL glass vials equipped with a Teflon seal, degassed with N_2, and heated to a 200 °C in an oil bath for 1 h. After reaction, the solutions were cooled to RT. The Teflon seals were pierced with a cannula where the other end was immersed in a stirred solution of 10 mL of 0.3% H_2O_2(aq) with a few drops of bromothylmol blue (as a pH indicator). Bubbling was observed with an instantaneous color change of solution (to yellow, indicating an acidic shift in pH) upon piercing the Teflon septum. An additional needle was inserted into the reaction vial with constant flowing N_2. After 10 min of sparging the solution, the flow was stopped. The solution containing H_2O_2 and indicator was back-titrated with a 0.01 M solution of KOH(aq) until the color returned to basic (blue in color). This was done in duplicate and averaged to give 110% ± 20% yield based on $Pt(bpym)Cl_2$ added.

■ ASSOCIATED CONTENT

Supporting Information

DFT coordinates, CIF files, supporting graphs and pictures, and further experimental details. This material is available free of charge via the Internet at http://pubs.acs.org.

■ AUTHOR INFORMATION

Corresponding Author

rperiana@scripps.edu

Notes

The authors declare no competing financial interest.

■ ACKNOWLEDGMENTS

The authors acknowledge the Center for Catalytic Hydrocarbon Functionalization, a DOE Energy Frontier Research Center (DOE DE-SC000-1298), for funding S.M.B., M.M.K., and B.G.H. Chevron Technology Corporation provided partial funding for O.A.M., V.R.Z., W.A.G., M.A., and R.A.P.

■ REFERENCES

(1) (a) Haggin, J. *Chem. Eng. News* **1993**, *71*, 23. (b) Arndtsen, B. A.; Bergman, R. G.; Mobley, T. A.; Peterson, T. H. *Acc. Chem. Res.* **1995**, *28*, 154. (c) Shilov, A. E.; Shul'pin, G. B. *Chem. Rev.* **1997**, *97*, 2879. (d) Periana, R. A.; Bhalla, G.; Tenn, W. J., III; Young, K. J. H.; Liu, X. Y.; Mironov, O.; Jones, C. J.; Ziatdinov, V. R. *J. Mol. Catal. A: Chem.* **2004**, *220*, 7. (e) Crabtree, R. H. *J. Org. Chem.* **2004**, *689*, 4083. (f) Conley, B. L.; Tenn, W. J., III; Young, K. J. H.; Ganesh, S. K.; Meier, S. K.; Ziatdinov, V. R.; Mironov, O.; Oxgaard, J.; Gonzales, J.; Goddard, W. A., III; Periana, R. A. *J. Mol. Catal. A: Chem.* **2006**, *251*, 8. (g) Hashiguchi, B. G.; Bischof, S. M.; Konnick, M. M.; Periana, R. A. *Acc. Chem. Res.* **2012**, *45*, 885.

(2) Gol'dschleger, N. F.; Es'kova, V. V.; Shilov, A. E.; Shteinman, A. A. *Russ. J. Phys. Chem.* **1972**, *46*, 785.

(3) (a) Shilov, A. E. *Activation of Saturated Hydrocarbons by Transition Metal Complexes*; Riedel: Dordrecht, 1984. (b) Shilov, A. E.; Shul'pin, G. B. *Activation and Catalytic Reactions of Saturated Hydrocarbons in the Presence of Metal Complexes*; Kluwer Academic: Dordrecht, 2000. (c) Shilov, A. E.; Shteinman, A. A. *Coord. Chem. Rev.* **1977**, *24*, 97.

(4) (a) Labinger, J. A.; Bercaw, J. E. *Nature* **2002**, *417*, 507. (b) Chen, G. S.; Labinger, J. A.; Bercaw, J. E. *Proc. Natl. Acad. Sci. U.S.A.* **2007**, *104*, 6915. (c) Rostovtsev, V. V.; Labinger, J. A.; Bercaw, J. E.; Lasseter, T.; Goldberg, K. I. *Organometallics* **1998**, *17*, 4530. (d) Rostovtsev, V. V.; Henling, L.; Labinger, J. A.; Bercaw, J. E. *Inorg. Chem.* **2002**, *41*, 3608. (e) Driver, T. G.; Williams, T. J.; Labinger, J. A.; Bercaw, J. E. *Organometallics* **2007**, *26*, 294. (f) Stahl, S. S.; Labinger, J. A. *J. Am. Chem. Soc.* **1995**, *117*, 9371. (g) Stahl, S. S.; Labinger, J. A.; Bercaw, J. E. *J. Am. Chem. Soc.* **1996**, *118*, 5961.

(5) (a) Fekl, U.; Goldberg, K. I. *Adv. Inorg. Chem.* **2003**, *54*, 259. (b) Wick, D. D.; Goldberg, K. I. *J. Am. Chem. Soc.* **1999**, *121*, 11900. (c) Pawlikowski, A. V.; Getty, A. D.; Goldberg, K. I. *J. Am. Chem. Soc.* **2007**, *129*, 10382. (d) Grice, K. A.; Goldberg, K. I. *Organometallics* **2009**, *28*, 953. (e) Vedernikov, A. N.; Binfield, S. A.; Zavalij, P. Y.; Khusnutdinova, J. R. *J. Am. Chem. Soc.* **2005**, *128*, 83. (f) Khusnutdi-

nova, J. R.; Zavalij, P. Y.; Vedernikov, A. N. *Organometallics* **2007**, *26*, 3466. (g) Vedernikov, A. N. *Curr. Org. Chem.* **2007**, *11*, 1401. (h) Yahav-Levi, A.; Goldberg, I.; Vigalok, A.; Vedernikov, A. N. *J. Am. Chem. Soc.* **2008**, *130*, 724. (i) Baik, M.-H.; Newcomb, M.; Friesner, R. A.; Lippard, S. J. *Chem. Rev.* **2003**, *103*, 2385. (j) Lieberman, R. L.; Rosenzwig, A. C. *Crit. Rev. Biochem. Mol.* **2004**, *39*, 147. (k) Sen, A. *Acc. Chem. Res.* **1998**, *31*, 550. (l) Butikofer, J. L.; Parson, T. G.; Roddick, D. M. *Organometallics* **2006**, *25*, 6108.

(6) (a) Luinstra, G. A.; Labinger, J. A.; Bercaw, J. E. *J. Am. Chem. Soc.* **1993**, *115*, 3004. (b) Luinstra, G. A.; Wang, L.; Stahl, S. S.; Stahl, J. A.; Labinger, J. A.; Bercaw, J. E. *Organometallics* **1994**, *13*, 755. (c) Luinstra, G. A.; Wang, L.; Stahl, S. S.; Labinger, J. A.; Bercaw, J. E. *J. Organomet. Chem.* **1995**, *504*, 75.

(7) Galus, Z. *Standard Potentials in Aqueous Solutuion*; Bard, A. J.; Parsons, R.; Jordan, J., Eds.; Marcel Dekker, Inc.: New York, 1985; pp 196−197.

(8) Emphasis in bold added by the authors.

(9) Comment in brackets added by the authors to clarify the statement.

(10) (a) Labinger, J. A.; Bercaw, J. E. *Top Organomet. Chem.* **2011**, *35*, 29. (b) Scollard, J. D.; Day, M.; Labinger, J. A.; Bercaw, J. E. *Hel. Chim. Acta* **2001**, *84*, 3247.

(11) A sampling of reviews on this topic: (a) Hashiguchi, B. G.; Hövelmann, C. H.; Bischof, S. M.; Lokare, K. S.; Leung, C.-H.; Periana, R. A. *Encyclopedia of Inorganic and Bioinorganic Chemistry: Energy Production and Storage*; Crabtree, R. H., Ed.; Wiley: Oxford, U.K., 2010, 101. (b) Lunsford, J. H. *Catal. Today* **2000**, *63*, 165. (c) Labinger, J. A. *Stud. Surf. Sci. Catal.* **2001**, *136*, 325. (d) Vedernikov, A. N. *Curr. Org. Chem.* **2007**, *11*, 1401. (e) Neufeldt, S. R.; Sanford, M. S. *Acc. Chem. Res.* **2012**, *45*, 936.

(12) Periana, R. A.; Taube, D. J.; Gamble, S.; Taube, H. Ligated platinum group metal catalyst complex and improved process for catalytically converting alkanes to esters and derivatives thereof. PTC International, 98/50333, Nov 6, 1998

(13) Periana, R. A.; Taube, D. J.; Gamble, S.; Taube, H.; Satoh, T.; Fujii, H. *Science* **1998**, *280*, 560.

(14) It could be considered that under the highly reactive conditions that the catalyst could be some highly active unligated Pt species. However, based on theoretical studies, the absence of Pt black (or other insoluble species) and the lack of catalysts observed when utilizing simple Pt salts as the Pt source make this unlikely.

(15) For representative examples of Pt^{IV} species with nitrogen based ligands see: (a) Shi, Y.; Li, S.-A.; Kerwood, D. J.; Goodisman, J.; Debrowaik, J. C. *J. Inorg. Biochem.* **2012**, *107*, 6. and references therein. (b) Miljković, D.; Poljarević, J. M.; Petković, F.; Blaževski, J.; Momčilović, M.; Nikolić, I.; Sakida, T.; Stošić-Grujičić, S.; Grgurić-Šipka, S.; Sabo, T. J. *Eur. J. Med. Chem.* **2012**, *47*, 194. and references therein. (c) Varbanov, H.; Valiahdi, S. M.; Legin, A. A.; Jakupec, M. A.; Roller, A.; Galanski, M.; Keppler, B. K. *Eur. J. Med. Chem.* **2011**, *46*, 5456 and references therein.

(16) Although a color change does not prove a change in oxidation state, Pt^{IV} species with nitrogen-based ligands are often yellow in color (see ref 15).

(17) Still, B. M.; Kumar, P. G. A.; Aldrich-Wright, J. R.; Price, W. S. *Chem. Soc. Rev.* **2007**, *36*, 665.

(18) Hristov, I. H.; Ziegler, T. *Organometallics* **2001**, *22*, 1668 We believe that the major part of the discrepancy is due to the fact that we include the energy of generating SO_3 from H_2SO_4 or $H_2S_2O_7$, which are the more stable forms of SO_3 in sulfuric acid.

(19) (a) Periana, R. A.; Mironov, O.; Taube, D.; Bhalla, G.; Jones, C. J. *Science* **2003**, *301*, 814. (b) Zerella, M.; Mukhopadhyay, S.; Bell, A. T. *Chem. Commun.* **2004**, 1948. (c) Gretz, E.; Oliver, T. F.; Sen, A. *J. Am. Chem. Soc.* **1987**, *109*, 8109. (d) Kao, L. C.; Hutson, A. C.; Sen, A. *J. Am. Chem. Soc.* **1991**, *113*, 700.

(20) (a) Jones, C. J.; Taube, D.; Ziatdinov, V. R.; Periana, R. A.; Nielsen, R. J.; Oxgaard, J.; Goddard, W. A., III. *Angew. Chem., Int. Ed.* **2004**, *43*, 4626. (b) De Vos, D. E.; Sels, B. F. *Angew. Chem., Int. Ed.* **2005**, *44*, 30. (c) Scott, V. J.; Labinger, J. A.; Bercaw, J. E. *Organometallics* **2010**, *29*, 4090. (c) Levchenko, L. A.; Sadkov, A. P.; Lariontseva, N. V.; Kulikova, V. S.; Shilova, A. K.; Shilov, A. E. *Doklady Biochem. Biophys.* **2004**, *394*, 33. Original Russian Text: *Dokl. Akad. Nauk* **2004**, *394*, 272. (d) Levchenko, L. A.; Kartsev, B. G.; Sadkov, A. P.; Shestakov, A. F.; Shilova, A. K.; Shilov, A. E. *Dokl. Akad. Nauk* **2007**, *412*, 35. (e) Pichugina, D. A.; Shestakov, A. F.; Kuz 'menko, N. E. *Russ. Chem. Bull., Int. Ed.* **2006**, *55*, 195. Original Russian Text: *Izv. Akad. Nauk. Ser. Khim.* **2006**, *2*, 191. (f) Pichugina, D. A.; Kuz 'menko, N. E.; Shestakov, A. F. *Gold Bull.* **2007**, *40*, 115. (g) Pichugina, D. A.; Shestakov, A. F.; Kuz'menko, N. E. *Russ. J. Phys. Chem. A* **2007**, *81*, 883. Original Russian Text: Pichugina, D. A.; Shestakov, A. F.; Kuz'menko, N. E. *Zh. Fiz. Khim.* **2007**, *81*, 1015.

(21) (a) Periana, R. A.; Taube, D.; Evitt, E. R.; Loffler, D. G.; Wentrcek, P. R.; Voss, G.; Masuda, T. *Science* **1993**, *259*, 340. (b) Gang, X.; Birch, H.; Zhu, Y.; Hjuler, H. A.; Bjerrum, N. J. *J. Catal.* **2000**, *196*, 287. (c) Sen, A.; Benvenuto, M. A.; Lin, M.; Hutson, A. C.; Basickes, N. *J. Am. Chem. Soc.* **1994**, *116*, 998. (d) Basickes, N.; Hogan, T. E.; Sen, A. *J. Am. Chem. Soc.* **1996**, *118*, 13111. (e) Snyder, J. C.; Grosse, A. V. US Patent 2493038, 1950. (f) Cundari, T. R.; Snyder, L. A.; Yoshikawa, A. *J. Mol. Struc.-Theochem.* **1998**, *425*, 13. (g) Cundari, T. R.; Yoshikawa, A. *J. Comput. Chem.* **1998**, *19*, 902. (h) Mukhopadhyay, S.; Bell, A. T. *J. Mol. Catal. A: Chem* **2004**, *211*, 59. (i) Mukhopadhyay, S.; Bell, A. T. *Adv. Synth. Catal.* **2004**, *346*, 913.

(22) (a) Lersch, M.; Tilset, M. *Chem. Rev.* **2005**, *105*, 2471. (b) Shulpin, G. B.; Shilov, A. E.; Kitaigorodskii, A. N.; Krevor, J. V. Z. J. *Organomet. Chem.* **1980**, *201*, 319. (c) Mamtora, J.; Crosby, S. H.; Newman, C. P.; Clarkson, G. J.; Rourke, J. P. *Organometallics* **2008**, *27*, 5559. (d) Newman, C. P.; Casey-Green, K.; Clarkson, G. J.; Cave, G. W. V.; Errington, W.; Rourke, J. P. *Dalton Trans.* **2007**, 3170. (e) Nizova, G. V.; Krevor, D. Z.; Kitaigorodskii, A. N.; Shul'pin, G. B. *Izv. Nats. Akad. Nauk SSSR., Ser. Khim* **1982**, *12*, 2805.

(23) Xu, X.; Fu, G.; Goddard, W. A., III; Periana, R. A. *Stud. Surf, Sci. Catal.* **2004**, *147*, 499.

(24) With a barrier of 41 kcal mol^{-1}, at 220 °C the system would have a TOF of 6.94×10^{-6} s^{-1} (see SI for calculation). This rate is more than 2 orders of magnitude slower than what we observe.

(25) Labinger, J. A.; Herring, A. M.; Lyon, D. K.; Luinstra, G. A.; Bercaw, J. E. *Organometallics* **1993**, *12*, 895.

(26) Note that the orders of these reactions in $[D_2SO_4]$ are not important, as the kinetic analysis is based on the assumption that the reactions of the model complex $(TFA)(X)Pt^{IV}$-CH_3 and X_2Pt^{IV}-CH_3 in the proposed Pathway B would show the same orders for $[D_2SO_4]$.

(27) DMSO was used as the solvent since *in situ* studies by NMR showed that **(TFA)XPt^{IV}-CH$_3$** is stable in this solvent for hours at RT. Additionally, control experiments showed that DMSO, with and without added $(bpym)PtCl_2$ and $(bpym)PtCl_4$, did not generate any CH_4 or CH_3OH upon addition to concentrated H_2SO_4 at 180 °C.

(28) This is because under conditions of low catalyst concentration and low levels of CH_4 conversion, the concentrations of H_2SO_4, H^+, and H_2O should remain constant. Importantly, this dependence would be independent of the value of k_4/k_{-4} or the solubility of SO_2 (as long as the system is not operating under diffusion control).

(29) Weinberg, D. A.; Labinger, J. A.; Bercaw, J. E. *Organometallics* **2007**, *26*, 167.

(30) The reaction is stopped immediately upon addition of **HO-Pt^{IV}-OH$_2$**.

(31) Ahlquist, M.; Periana, R. A.; Goddard, W. A. *Chem. Commun.* **2009**, *17*, 2373.

(32) Bacells, D.; Clot, E.; Eisenstein, O. *Chem. Rev.* **2010**, *110*, 749.

(33) (a) Kiernan, P. M.; Ludi, A. *J. Chem. Soc. Dalton* **1978**, 1127. (b) Connick, W. B.; Marsh, R. E.; Schaefer, W. P.; Gray, H. B. *Inorg. Chem.* **1997**, *36*, 913. (c) Bruce, J.; Johnson, D.; Cordes, W.; Sadoski, R. *J. Chem. Crystallogr.* **1997**, *27*, 695.

(34) Bancroft, D. P.; Cotton, F. A.; Falvello, L. R.; Schwotzer, W. *Inorg. Chem.* **1986**, *25*, 763.

(35) Compound synthesis was previously reported in: Otoo, S.; Roodt, A. *J. Organomet. Chem.* **2006**, *691*, 4626.

(36) Scott, J. D.; Pudephatt, R. J. *Organometallics* **1986**, *5*, 1538.

(37) For the Microsoft Excel deconvolution tables see the supporting information of: Young, K. J. H.; Meier, S. K.; Gonzales, J. M.; Oxgaard, J.; Goddard, W. A., III; Periana, R. A. *Organometallics* **2006**, *25*, 4734.